

# When Confidence Misleads: Suffix Anchoring and Anchor-Proximity Confidence Modulation for Diffusion Language Models

Jungwon Park<sup>1,5</sup>, Jimyeong Kim<sup>2</sup>, Jungmin Ko<sup>3</sup>, Nojun Kwak<sup>3,4</sup>, Wonjong Rhee<sup>3,4</sup>

<sup>1</sup>RICS, <sup>2</sup>AIIS, <sup>3</sup>IPAI, <sup>4</sup>Department of Intelligence and Information,  
Seoul National University

<sup>5</sup>Daegu Gyeongbuk Institute of Science and Technology

{quoded97, wlaud1001, jungminko, nojunk, wrhee}@snu.ac.kr

## Abstract

Diffusion language models decode text by iteratively denoising masked token sequences, making the choice of which positions to decode a central inference-time decision. Most training-free decoding strategies use model confidence for position selection, assuming that high-confidence positions are ready to be decoded. In this work, we revisit this assumption by studying when confidence misleads fully non-autoregressive (fully non-AR) decoding. EOT tokens can receive high confidence and cause incomplete generation; inserting a suffix anchor can mitigate this issue but introduces local overconfidence near the anchor, causing anchor-adjacent tokens to be decoded too early. To address these issues, we propose **Suffix-Anchored Confidence Modulation**, a simple training-free method that inserts a short suffix anchor to encourage response completion and modulates confidence near the anchor according to decoding progress. This preserves the response-completion benefit of suffix anchoring while reducing premature decoding of anchor-adjacent tokens. Across text-only reasoning, vision-language reasoning, and code-generation benchmarks, our method consistently improves confidence-based fully non-AR decoding, outperforms explicit EOT suppression, and preserves the parallel decoding advantage of fully non-AR generation.

## 1 Introduction

Diffusion Language Models (DLMs) generate text by iteratively denoising masked token sequences, allowing multiple positions to be decoded in parallel rather than generating one token at a time from left to right (Lou et al., 2023; Shi et al., 2024; Sahoo et al., 2024; Zheng et al., 2025; Ou et al., 2025). While this enables flexible non-autoregressive generation, it also introduces a key inference-time challenge: at each denoising step, the model must decide not only what tokens to predict, but also which masked positions to decode.

Most training-free DLM decoding strategies use model confidence as the position-selection signal. For example, *top-probability decoding* (Chang et al., 2022; Nie et al., 2026), also commonly referred to as *low-confidence remasking*, selects positions whose predicted tokens have the highest probability, while *top-margin decoding* (Kim et al., 2025b) selects positions whose top predictions are well separated. Although simple and effective, these strategies implicitly assume that high confidence indicates that a position is ready to be decoded at the current step. In this work, we revisit this assumption in fully non-autoregressive (fully non-AR) DLM decoding.

Recent work has revealed a failure mode of this assumption: *instruction-tuned DLMs may assign high confidence to end-of-text (EOT) tokens, leading to incomplete or extremely short outputs in fully non-AR decoding* (Nie et al., 2026). Existing approaches address this issue with explicit EOT suppression (Nie et al., 2026), model adaptation (Kim et al., 2025a), or semi-autoregressive (semi-AR) decoding (Arriola et al., 2025; Cheng et al., 2025; Wu et al., 2025). However, these approaches either introduce token-specific suppression, require additional training, or partially give up the flexibility of fully non-AR generation.

A simple alternative is to provide weak structural guidance at inference time. Specifically, before decoding begins, we insert a short suffix anchor near the end of the response region, such as “*The answer is*” for reasoning tasks or return for code generation. This anchor signals that meaningful content should continue toward a later response region, discouraging premature EOT generation without explicitly suppressing EOT tokens. We find that suffix anchoring substantially reduces incomplete generation. However, it also introduces a new failure mode in confidence-dynamics: *suffix anchors can induce misleadingly high confidence around the anchor before sufficient preceding context has*

*been generated*. As a result, confidence-based decoding may unmask anchor-adjacent tokens too early, often producing inaccurate outputs despite high confidence. In reasoning tasks, this can produce final answers before the reasoning context is sufficiently developed; in code-generation, it can similarly decode anchor-adjacent code before the surrounding function logic is adequately formed.

To address this problem, we propose **Suffix-Anchored Confidence Modulation**, a simple training-free method that combines suffix anchoring with anchor-proximity confidence modulation. The confidence modulation down-weights confidence scores near the suffix anchor early in decoding and gradually restores them as decoding progresses. This preserves the response-completion benefit of suffix anchoring while reducing early inaccurate decoding of anchor-adjacent tokens. The method requires no model training, auxiliary modules, or architectural modification, and is directly applicable to standard confidence-based decoding strategies in a plug-and-play manner.

We evaluate our method across text-only reasoning, vision-language reasoning, and code-generation benchmarks. On LLaDA (Nie et al., 2026) and Dream (Ye et al., 2025), our method consistently improves fully non-AR decoding on GSM8K (Cobbe et al., 2021), MATH-500 (Hendrycks et al., 2021; Lightman et al., 2024), StrategyQA (Geva et al., 2021), and MMLU-Pro (Wang et al., 2024). On LaViDa (Li et al., 2026), the gains extend to vision-language reasoning benchmarks such as MathVista (Lu et al., 2024) and ChartQA (Masry et al., 2022). We further show that our method outperforms explicit EOT suppression without directly prohibiting EOT tokens, and improves over the semi-AR decoding, with larger gains under limited step budgets where fully non-AR parallelism becomes especially valuable.

## 2 Related Work

### 2.1 Diffusion Language Models

Diffusion models have achieved strong generative performance in continuous domains such as image and video generation (Sohl-Dickstein et al., 2015; Ho et al., 2020; Song et al., 2020; Karras et al., 2022; Peebles and Xie, 2023; Ho et al., 2022). Motivated by this progress, prior work has extended diffusion to discrete text generation through categorical corruption processes, discrete-state Markov chains, and continuous-time variants (Hoogeboom

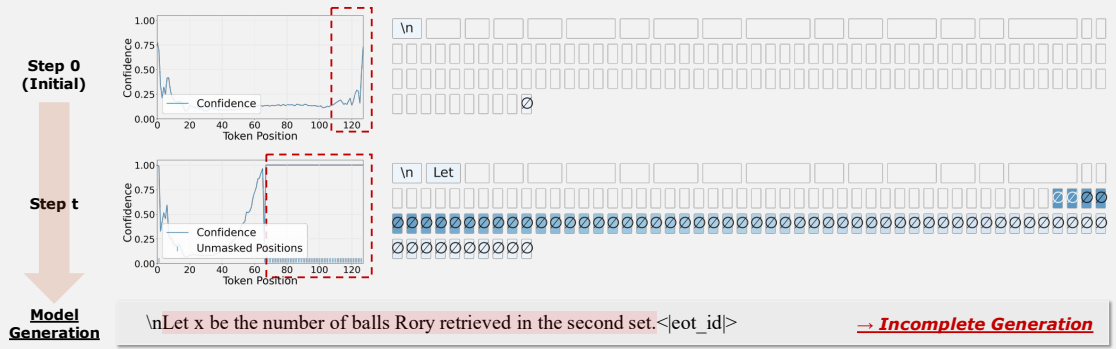
et al., 2021; Austin et al., 2021a; Campbell et al., 2022). Subsequent studies developed masked diffusion language models and clarified connections among different parameterizations (Lou et al., 2023; Shi et al., 2024; Sahoo et al., 2024; Zheng et al., 2025; Ou et al., 2025). Recent large-scale DLMs, including LLaDA (Nie et al., 2026) and Dream (Ye et al., 2025), demonstrate that masked denoising can scale to 7–8B-scale language models, achieving performance comparable to similar-scale autoregressive LLMs while supporting flexible and parallel token generation. Meanwhile, semi-AR decoding generates text blocks in a left-to-right order while applying diffusion-style parallel decoding within each block, enabling stable and efficient inference but restricting position selection to the block being generated (Arriola et al., 2025; Cheng et al., 2025; Wu et al., 2025). Our work focuses on fully non-AR decoding, where masked positions can be selected anywhere in the response region, making the unmasking policy especially critical.

### 2.2 Confidence-Based Decoding in DLMs

A standard training-free strategy for DLM decoding is to use confidence as the position-selection signal, as in top-probability decoding and related variants such as top-margin decoding (Chang et al., 2022; Kim et al., 2025b; Nie et al., 2026). Recent work also uses confidence for inference-time acceleration and scheduling. Fast-dLLM (Wu et al., 2025) accelerates DLM inference while limiting quality degradation by applying a confidence threshold and unmasking only positions with sufficiently high prediction confidence. Prophet (Li et al., 2025) observes early answer convergence in DLM trajectories and uses probability gaps between answer candidates to decide when decoding can stop early. ICE (Jin et al., 2025) uses in-place chain-of-thought prompting and confidence-aware early exit to improve DLM inference. AdaBlock-dLLM (Lu et al., 2025) analyzes confidence dynamics in semi-AR decoding and adaptively adjusts block sizes according to semantic boundary confidence. Together, these works show that confidence is a useful signal for DLM inference. Our work studies a complementary aspect of confidence-based decoding: when and how confidence can mislead position selection in fully non-AR generation, focusing on EOT overconfidence and anchor-induced local overconfidence. We address these issues with a simple training-free modification of standard confidence-based decoding strategies.

**Question :** Rory is retrieving tennis balls from the court after a tennis match. In the first of three sets, he had to retrieve four more balls than in the second set. In the third set, he retrieved half as many balls as in the second. He retrieved 19 tennis balls in all. How many tennis balls did he retrieve in the first set of the match?  
**Reference Answer : 10**

**Failure Mode 1 : EOT Overconfidence in Naive Decoding**



**Failure Mode 2 : Anchor-Induced Local Overconfidence**

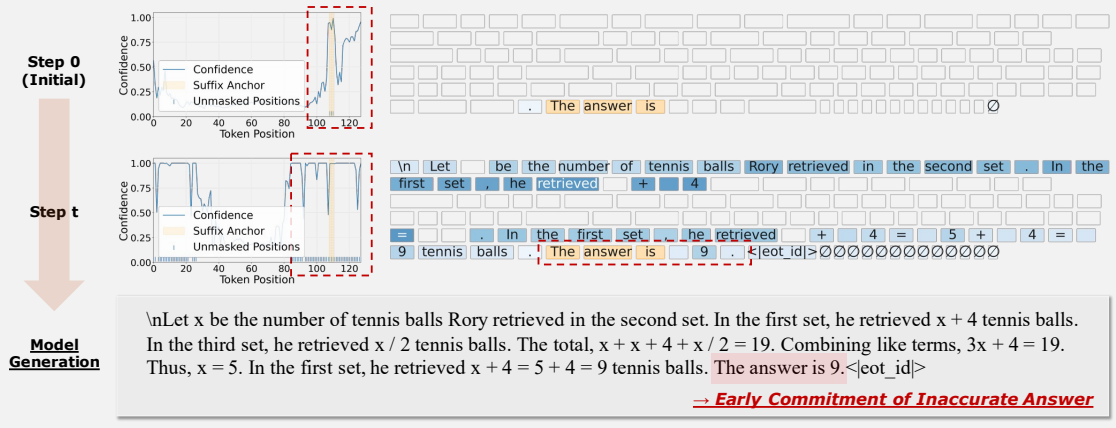


Figure 1: **Two failure modes of confidence-based position selection.** Top: naive confidence-based decoding assigns high confidence to EOT tokens and unmarks them before the response is sufficiently generated, resulting in incomplete output. Bottom: suffix anchoring improves response completion but induces misleadingly high confidence near the anchor, causing anchor-adjacent tokens to be decoded too early and producing an incorrect final answer. Darker blue token boxes indicate positions decoded at later steps. ∅ denotes the <|endof text|> token.

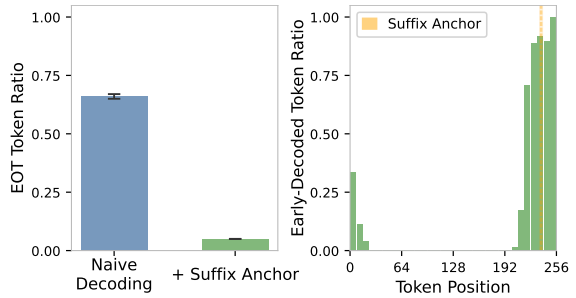


Figure 2: **Effects of suffix anchoring.** Left: suffix anchoring reduces the EOT token ratio in generated outputs, mitigating incomplete generation. Right: under suffix-anchored decoding, tokens decoded within the first 15% of steps concentrate near the suffix anchor. The 256-token response region is divided into 32 bins, and each bar reports the average fraction of decoded tokens in the corresponding bin. Yellow vertical lines indicate the suffix-anchor positions. All results are computed on the GSM8K (Cobbe et al., 2021) test split.

**3 When Confidence Misleads Position Selection**

Confidence-based decoding uses model confidence to select masked positions for decoding. This selection is especially critical in fully non-AR decoding, where positions can be selected anywhere in the response region without the left-to-right block order imposed by semi-AR decoding. Consequently, high-confidence positions may be decoded before their supporting context is sufficiently resolved. We analyze two representative failure modes of this behavior. The first is a recently studied failure mode in which EOT tokens receive high confidence and cause incomplete or extremely short generations (Kim et al., 2025a; Nie et al., 2026). The second is an anchor-induced failure mode, where suffix anchors improve response completion but create misleadingly high confidence around

anchor-adjacent positions. Unless otherwise specified, analyses in this section use top-probability decoding as the base decoding strategy.

**Failure mode 1: EOT overconfidence in naive decoding.** In naive fully non-AR decoding, EOT tokens near the end of the response region can receive high confidence early in the decoding process. As shown in Figure 1, confidence-based decoding may then unmask these positions before the response is sufficiently generated, resulting in incomplete outputs. This phenomenon has been reported in recent work (Kim et al., 2025a; Nie et al., 2026); here, we use it as a motivating example where high confidence does not necessarily indicate that a position is ready to be decoded.

**Suffix anchoring mitigates incomplete generation.** A simple way to reduce incomplete generation is to provide weak structural guidance at inference time. Before decoding begins, we insert a short suffix anchor near the end of the response region, using “*The answer is*” for reasoning tasks. The anchor signals that meaningful content should continue toward a later response region, thereby discouraging premature EOT generation without explicitly suppressing EOT tokens. This effect is shown in Figure 2, where adding a suffix anchor substantially reduces the average EOT ratio in generated outputs. Importantly, the suffix anchor is not intended to impose a fixed response template, but to provide a lightweight cue for response continuation, as further supported by the anchor-choice and anchor-position ablations in Appendices C.2–C.3.

**Failure mode 2: Anchor-induced local overconfidence.** While suffix anchoring mitigates incomplete generation, it also changes the local confidence landscape around the anchor. As shown in Figure 1, anchor-adjacent positions can become misleadingly confident before sufficient preceding context has been generated. Confidence-based decoding may then unmask tokens near the anchor too early, producing inaccurate tokens despite high confidence. This behavior is also supported by Figure 2, which shows that during the first 15% of decoding steps, a disproportionately large fraction of decoded positions lies near the suffix anchor. This early concentration of decoded positions near the anchor suggests that suffix anchoring can bias confidence-based position selection toward the anchor region before the supporting context is sufficiently resolved.

**Summary.** We find that suffix anchoring mitigates EOT-induced incomplete generation, but can also bias confidence-based position selection toward the anchor region too early. This motivates our method, which preserves the response-completion benefit of suffix anchoring while reducing early inaccurate anchor-adjacent decoding through anchor-proximity confidence modulation.

## 4 Method

We propose Suffix-Anchored Confidence Modulation, a simple training-free modification of standard confidence-based decoding. The method has two components. First, we insert a short suffix anchor to reduce EOT-induced incomplete generation. Second, we down-weight confidence scores near the suffix anchor early in decoding and gradually restore them as decoding progresses, reducing premature decoding of anchor-adjacent positions. Figure 3 compares standard confidence-based decoding, suffix anchoring, and the full method with confidence modulation. The complete decoding procedure is outlined in Algorithm 1 in Appendix A.

**DLM decoding preliminaries.** Let  $\mathbf{x}^{(t)} = (x_1^{(t)}, \dots, x_L^{(t)})$  be the partially decoded response at decoding step  $t$ , where  $L$  is the response length and unresolved positions are represented by [MASK]. Let  $\mathcal{M}^{(t)} = \{i : x_i^{(t)} = \text{[MASK]}\}$  be the set of masked positions. At each step, the DLM predicts a token distribution over each masked position,

$$p_{\theta}(\cdot \mid \mathbf{x}^{(t)}, i), \quad i \in \mathcal{M}^{(t)}. \quad (1)$$

A confidence-based decoding strategy assigns each masked position  $i$  a confidence score  $c_i^{(t)}$ , such as the maximum predicted token probability in top-probability decoding or the gap between the top two predicted probabilities in top-margin decoding. The strategy then unmask a subset of high-confidence positions. Our method reweights  $c_i^{(t)}$  after it is computed, so the same formulation applies to different choices of confidence score.

**Suffix anchoring.** Before decoding, we insert a short suffix anchor near the end of the response region. The anchor is designed to provide a lightweight continuation cue toward a later response region, rather than prescribe a detailed response structure. It can be a short phrase such as “*The answer is*”, or even a minimal token such as “.” or “,”, as discussed in Appendix C.2. Let  $\mathcal{A}$  denote the set of positions corresponding to the inserted

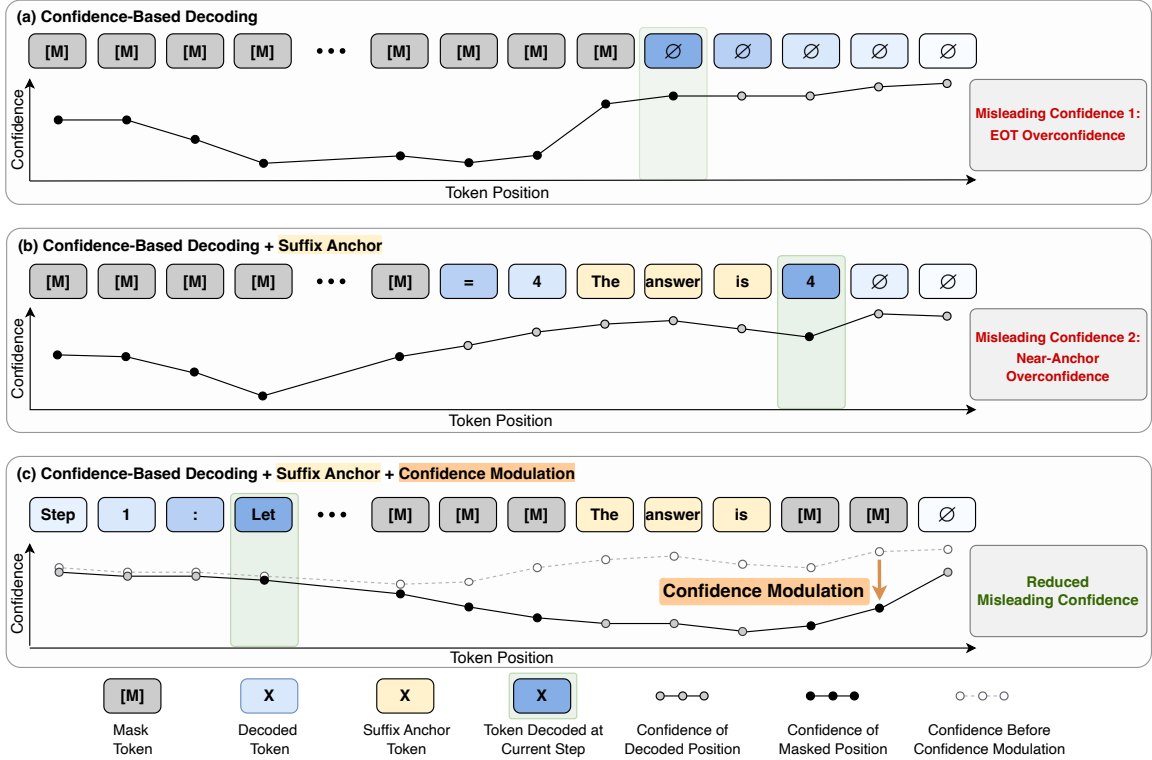


Figure 3: **Overview of Suffix-Anchored Confidence Modulation.** (a) Standard confidence-based decoding can select high-confidence EOT tokens too early. (b) Adding a suffix anchor reduces EOT overconfidence but may induce misleadingly high confidence near the anchor. (c) Our method applies anchor-proximity confidence modulation to reduce premature decoding of anchor-adjacent positions while preserving the benefit of suffix anchoring. Darker blue token boxes indicate positions decoded at later steps.  $\emptyset$  denotes the  $\langle \text{end of text} \rangle$  token.

anchor tokens. This minimal design preserves the flexibility of free-form generation while reducing incomplete generation caused by premature EOT decoding.

**Anchor-proximity weight.** To down-weight confidence near the suffix anchor, we define an anchor-proximity weight for each token position  $i$ :

$$w_i = \min \left\{ 1, \beta \max_{a \in \mathcal{A}} \exp \left( -\frac{|i - a|}{\kappa} \right) \right\}. \quad (2)$$

Here,  $\kappa > 0$  controls the spatial decay from the anchor and  $\beta > 0$  controls the overall modulation strength. Positions closer to the suffix anchor receive larger weights and are therefore more strongly affected by the confidence reweighting. The clipping by 1 keeps the modulation bounded.

**Progress-dependent confidence modulation.** Anchor-induced overconfidence is most problematic early in decoding, when little preceding context has been resolved. As decoding progresses, more tokens are unmasked, and anchor-adjacent predictions become conditioned on richer surrounding context. We therefore down-weight confidence near the suffix anchor and gradually relax

this down-weighting as decoding progresses. Let  $m^{(t)} = |\mathcal{M}^{(t)}|$  be the number of masked positions at step  $t$ . We define decoding progress as

$$p^{(t)} = 1 - \frac{m^{(t)}}{L}, \quad (3)$$

where larger values indicate later decoding stages. Given the original confidence score  $c_i^{(t)}$  from the underlying decoding strategy, we compute the reweighted confidence score as

$$\tilde{c}_i^{(t)} = c_i^{(t)} \left( 1 - w_i(1 - p^{(t)})^\gamma \right), \quad (4)$$

where  $\gamma > 0$  controls how quickly the down-weighting is relaxed. Early in decoding,  $(1 - p^{(t)})^\gamma$  is large, so confidence near the suffix anchor is down-weighted more strongly. As decoding progresses, this factor decreases toward zero, and  $\tilde{c}_i^{(t)}$  approaches the original confidence  $c_i^{(t)}$ . This reduces premature decoding of anchor-adjacent positions while recovering the base confidence-based decoding behavior in later stages.

**Position selection.** At each decoding step, the underlying decoding strategy computes a base confidence score  $c_i^{(t)}$  for each masked position. We

Model	Decoding Method	Math Reasoning		Commonsense Reasoning	Broad Knowledge Reasoning	Average
		GSM8K	MATH-500	StrategyQA	MMLU-Pro	
LLaDA	Random	47.16	18.00	58.81	34.26	39.56
	Top Probability	14.94	14.60	19.65	35.23	21.11
	+ Suffix Anchor	49.89	21.80	66.52	37.92	44.03
	+ Confidence Modulation	<b>76.88</b>	<b>29.00</b>	<b>70.45</b>	<b>39.19</b>	<b>53.88</b>
	Top Margin	14.78	16.20	28.53	36.39	23.98
	+ Suffix Anchor	56.18	22.40	66.08	38.30	45.74
	+ Confidence Modulation	<b>72.33</b>	<b>25.40</b>	<b>68.12</b>	<b>38.42</b>	<b>51.07</b>
Dream	Random	39.27	6.60	69.43	39.22	38.63
	Top Probability	38.29	12.40	56.91	38.52	36.53
	+ Suffix Anchor	36.39	23.20	74.24	47.85	45.42
	+ Confidence Modulation	<b>49.13</b>	<b>30.80</b>	<b>75.40</b>	<b>48.83</b>	<b>51.04</b>
	Top Margin	43.67	13.40	62.45	43.38	40.73
	+ Suffix Anchor	41.70	23.60	75.98	48.39	47.42
	+ Confidence Modulation	<b>48.60</b>	<b>28.60</b>	<b>76.13</b>	<b>49.40</b>	<b>50.68</b>

Table 1: **Results on text-only reasoning benchmarks.** Accuracy (%) is reported on four text-only reasoning benchmarks using LLaDA 8B-Instruct and Dream 7B-Instruct. For each confidence-based decoding strategy, the unmodified baseline, suffix anchoring, and the full method (suffix anchoring with confidence modulation) are compared. Random position selection is included as a non-confidence-based reference. **Bold** indicates the best result within each confidence-based decoding group.

replace this score with the reweighted score  $\tilde{c}_i^{(t)}$  before selecting positions to unmask. The selected positions are then filled with the tokens predicted by the DLM. Since our method only inserts a suffix anchor and reweights scalar confidence scores during decoding, it requires no model training, auxiliary modules, or architectural changes, and can be readily incorporated into standard confidence-based DLM decoding strategies.

## 5 Experiments

### 5.1 Experimental Setup

**Models and benchmarks.** We evaluate our method on two representative text-only DLMs, LLaDA 8B-Instruct (Nie et al., 2026) and Dream 7B-Instruct (Ye et al., 2025), and one vision-language DLM, LaViDa-Instruct (Li et al., 2026). For text-only reasoning, we use GSM8K (Cobbe et al., 2021) and MATH-500 (Hendrycks et al., 2021; Lightman et al., 2024) for mathematical reasoning, StrategyQA (Geva et al., 2021) for commonsense reasoning, and MMLU-Pro (Wang et al., 2024) for broad-domain knowledge reasoning. For vision-language reasoning, we use MathVista (Lu et al., 2024) and ChartQA (Masry et al., 2022). We additionally evaluate code generation on HumanEval (Chen et al., 2021) and MBPP (Austin et al., 2021b). We use 5-shot prompting for MMLU-Pro, 3-shot prompting for MBPP, and zero-shot prompting for all other benchmarks. We report

Model	Decoding Method	MathVista	ChartQA	Average
LaViDa	Random	28.80	27.12	27.96
	Top Probability	27.00	24.12	25.56
	+ Suffix Anchor	29.10	44.96	37.03
	+ Confidence Modulation	<b>34.60</b>	<b>45.92</b>	<b>40.26</b>
	Top Margin	24.80	23.24	24.02
	+ Suffix Anchor	29.20	45.08	37.14
	+ Confidence Modulation	<b>33.20</b>	<b>45.44</b>	<b>39.32</b>

Table 2: **Results on vision-language reasoning benchmarks.** Accuracy (%) is reported on MathVista and ChartQA using LaViDa-Instruct. For each confidence-based decoding strategy, the unmodified baseline, suffix anchoring, and the full method with confidence modulation are compared. **Bold** indicates the best result within each confidence-based decoding group.

accuracy for reasoning benchmarks and pass@1 for code-generation benchmarks.

**Decoding methods.** We evaluate two confidence-based fully non-AR decoding strategies: top-probability and top-margin decoding. For each, we compare the unmodified baseline, the baseline with suffix anchoring, and the full method with confidence modulation. We report random position selection as a non-confidence-based reference.

**Implementation details.** We use generation length  $L = 256$  for GSM8K and MATH-500, and  $L = 128$  for the remaining benchmarks. Unless otherwise specified, the number of decoding steps is set to  $T = L/2$ . The suffix anchor is placed 20 positions before the end of the response region,

Base Decoding	Modification	Text-Only Reasoning				Vision-Language Reasoning		Average
		GSM8K	MATH-500	StrategyQA	MMLU-Pro	MathVista	ChartQA	
Top Probability	None	14.94	14.60	19.65	35.23	27.00	24.12	22.59
	EOT Suppression	52.39	20.80	64.05	37.83	30.40	33.20	39.78
	Ours	<b>76.88</b>	<b>29.00</b>	<b>70.45</b>	<b>39.19</b>	<b>34.60</b>	<b>45.92</b>	<b>49.34</b>
Top Margin	None	14.78	16.20	28.53	36.39	24.80	23.24	23.99
	EOT Suppression	55.04	22.80	65.36	38.33	32.90	34.52	41.49
	Ours	<b>72.33</b>	<b>25.40</b>	<b>68.12</b>	<b>38.42</b>	<b>33.20</b>	<b>45.44</b>	<b>47.15</b>

Table 3: **Comparison with explicit EOT suppression.** Explicit EOT suppression and our method are compared on text-only reasoning benchmarks with LLaDA and vision-language reasoning benchmarks with LaViDa. “None” denotes the unmodified base decoding strategy. **Bold** indicates the best result within each base decoding group.

Decoding Method	Step Budget			
	$T = 32$	$T = 64$	$T = 128$	$T = 256$
Fully Non-AR	32.52	26.46	14.94	2.96
+ Suffix Anchor	45.11	48.22	49.89	54.97
+ Confidence Modulation	<b>57.70</b>	<b>69.67</b>	<b>76.88</b>	<b>77.41</b>
Semi-AR, block size = 8	11.37	56.71	72.33	74.07
Semi-AR, block size = 16	21.15	60.96	73.39	74.07
Semi-AR, block size = 32	29.72	63.31	72.25	73.01
Semi-AR, block size = 64	36.32	63.46	72.18	71.87

Table 4: **Comparison with semi-AR decoding under different step budgets.** Fully non-AR and semi-AR decoding are compared on GSM8K using LLaDA with generation length  $L = 256$ . Top-probability decoding is used as the base position-selection strategy. For each step budget  $T$ , all methods unmask  $L/T$  tokens per step. **Bold** indicates the best result for each step budget.

leaving most of the response budget before the anchor for free-form generation. We use “*The answer is*” as the suffix anchor for reasoning tasks and return for code generation. Additional implementation details are provided in Appendix B.

**Hyperparameters.** Our method uses three hyperparameters:  $\kappa$ ,  $\beta$ , and  $\gamma$ . We select them with a lightweight sweep over  $\kappa \in \{12, 14\}$ ,  $\beta \in \{1.0, 1.1, 1.2, 1.3, 1.4, 1.5\}$ , and  $\gamma \in \{0.7, 0.85, 1.0\}$  on a small subset of 128 samples from the training or validation split when available. The sweep is conducted with LLaDA under top-probability decoding, and the selected values are reused for top-margin decoding and Dream on the same benchmark. When no training or validation split is available, we use the GSM8K setting,  $(\kappa, \beta, \gamma) = (14, 1.3, 0.85)$ . Details, including sensitivity analysis, are provided in Appendix B.3.

## 5.2 Main Results

**Text-only reasoning.** Table 1 reports results on four text-only reasoning benchmarks using LLaDA and Dream. Across both models, suffix anchoring substantially improves confidence-based fully non-

AR decoding in most settings. The full method with confidence modulation further improves the average performance for every model–decoding pair. For LLaDA, the average score increases from 21.11 to 53.88 under top-probability decoding and from 23.98 to 51.07 under top-margin decoding. For Dream, the average score increases from 36.53 to 51.04 under top-probability decoding and from 40.73 to 50.68 under top-margin decoding. The improvements are especially large on math reasoning benchmarks, where the base confidence-based strategies often suffer from incomplete generation. For example, on GSM8K, our method improves LLaDA from 14.94 to 76.88 under top-probability decoding and from 14.78 to 72.33 under top-margin decoding. The gains are not limited to math benchmarks: on StrategyQA and MMLU-Pro, the full method also improves over the baselines for both LLaDA and Dream.

**Vision-language reasoning.** Table 2 evaluates LaViDa on MathVista and ChartQA. A similar trend appears in the vision-language setting: suffix anchoring gives a large improvement over the confidence-based baseline, and confidence modulation provides a further gain. Averaged across the two benchmarks, our method improves top-probability decoding from 25.56 to 40.26 and top-margin decoding from 24.02 to 39.32. The gains are especially pronounced on ChartQA, where our method improves top-probability decoding from 24.12 to 45.92 and top-margin decoding from 23.24 to 45.44.

Overall, these results show that suffix anchoring with confidence modulation consistently improves confidence-based fully non-AR decoding across models, decoding strategies, and both text-only and vision-language reasoning tasks. Additional code-generation results on HumanEval and MBPP are provided in Table 11 of Appendix C.1.

Method	Accuracy
Ours w/o Progress Dependence	72.25
Ours	<b>76.88</b>

Table 5: **Ablation of progress dependence in confidence modulation.**

### 5.3 Comparisons with EOT Suppression and Semi-AR Decoding

We compare our method with two alternative decoding methods. Explicit EOT suppression (Nie et al., 2026) prohibits EOT generation by setting the confidence of EOT tokens to negative infinity, while semi-AR decoding constrains generation to proceed block by block. In contrast, our method preserves fully non-AR position selection and does not directly prohibit EOT tokens.

**Comparison with EOT suppression.** Table 3 shows that EOT suppression substantially improves over the unmodified confidence-based baselines, supporting that EOT overconfidence is as an important failure mode. However, our method consistently outperforms EOT suppression across text-only and vision-language reasoning benchmarks. This indicates that suffix anchoring with confidence modulation provides a more effective alternative to directly suppressing EOT tokens.

**Comparison with semi-AR decoding.** Table 4 compares our method with semi-AR decoding under different step budgets and block sizes. Our method outperforms all semi-AR configurations across all step budgets. The advantage is especially large under limited step budgets, where fewer decoding steps require more tokens to be unmasked per step and flexible parallel position selection becomes especially important: at  $T = 32$ , our method achieves 57.70, compared with the best semi-AR result of 36.32. These results show that our method improves fully non-AR decoding while preserving its parallel decoding advantage, whereas semi-AR decoding partially sacrifices this advantage by imposing block-wise generation.

### 5.4 Ablation Studies and Efficiency Analysis

We conduct ablation studies and efficiency analysis on GSM8K using LLaDA 8B-Instruct with top-probability decoding. Table 5 evaluates the effect of the progress-dependent factor  $(1 - p^{(t)})^\gamma$  in Eq. (4). Without this factor, the anchor-proximity confidence down-weighting remains fixed throughout decoding, which reduces accuracy from 76.88 to 72.25. This shows that gradually relaxing the

Decoding Method	Generation Length		
	$L = 64$	$L = 128$	$L = 256$
Top Probability	39.35	23.58	14.94
+ Suffix Anchor	51.55	56.94	49.89
+ Confidence Modulation	<b>62.55</b>	<b>75.82</b>	<b>76.88</b>

Table 6: **Ablation over generation length.** Generation length is varied over  $L \in \{64, 128, 256\}$ , with the decoding step budget set to  $T = L/2$ .

Decoding Method	Throughput $\uparrow$	Latency $\downarrow$
Top Probability	25.02	10.23
+ Suffix Anchor	25.03	10.23
+ Confidence Modulation	24.93	10.27

Table 7: **Inference efficiency.** Throughput (tokens/s) is the average number of generated tokens per second, and latency (s/sample) is the average inference time per sample. All measurements are taken on a single NVIDIA A6000 GPU.

confidence down-weighting as decoding progresses is beneficial. Table 6 reports results across different generation lengths, with the step budget set to  $T = L/2$ . Suffix anchoring improves upon the unmodified baseline across all generation lengths, and the full method with confidence modulation further improves performance in every setting. Table 12 in Appendix C.2 studies the effect of suffix anchor choice, showing that our method remains robust across different suffix anchors; even the anchor “.”, which provides minimal response structure, achieves 74.68, close to 76.88 with the default anchor. Finally, Table 7 reports inference throughput and latency. Suffix anchoring and confidence modulation introduce negligible overhead compared with the baseline: throughput remains around 25.0 tokens/s and latency remains around 10.2 s/sample for all three decoding variants. This shows that our method improves decoding quality without sacrificing inference efficiency.

## 6 Conclusion

In this work, we studied how confidence-based position selection can mislead fully non-AR DLM decoding, leading to EOT-induced incomplete generation or anchor-induced local overconfidence. We proposed Suffix-Anchored Confidence Modulation, a simple training-free method that combines suffix anchoring with anchor-proximity confidence modulation. Across text-only reasoning, vision-language reasoning, and code-generation benchmarks, our method consistently improves confidence-based decoding while preserving the parallel decoding advantage of fully non-AR generation.

## Limitations

Our method is a training-free modification to confidence-based decoding and therefore does not update model parameters or address errors caused by insufficient model knowledge or reasoning ability. It is most useful when confidence-based position selection is a major source of failure, and may provide smaller gains when errors arise from incorrect token predictions rather than premature or suboptimal position selection.

For simplicity, the main experiments use fixed suffix anchors and a predefined anchor position. However, Table 12 in Appendix C.2 shows that our method remains robust across different suffix anchor choices, and Table 13 in Appendix C.3 shows that it also remains robust across different anchor positions within the later response region. While these two ablations indicate robustness to anchor form and placement, the optimal anchor form or placement may still vary across tasks and output formats. In addition, confidence modulation introduces a small number of hyperparameters, which we tune with a lightweight sweep and reuse across settings when possible. More adaptive strategies for automatically choosing anchors, anchor placements, and modulation strengths would be a valuable direction for future work.

Finally, our experiments focus on representative text-only and vision-language DLMs using standard reasoning and code-generation benchmarks. Further evaluation on multilingual tasks and more diverse multimodal settings would be valuable.

## Acknowledgments

This work was supported by Institute of Information & communications Technology Planning & Evaluation (IITP) grant funded by the Korea government (MSIT) ([NO.RS-2021-II211343, Artificial Intelligence Graduate School Program (Seoul National University)], [No.RS-2023-00235293, Development of autonomous driving big data processing, management, search, and sharing interface technology to provide autonomous driving data according to the purpose of usage]) and the InnoCORE program of the Ministry of Science and ICT (26-InnoCORE-01).

## References

Marianne Arriola, Aaron Gokaslan, Justin Chiu, Zhihan Yang, Zhixuan Qi, Jiaqi Han, Subham Sahoo, and

Volodymyr Kuleshov. 2025. Block diffusion: Interpolating between autoregressive and diffusion language models. In *International Conference on Learning Representations*, volume 2025, pages 50726–50753.

Jacob Austin, Daniel D Johnson, Jonathan Ho, Daniel Tarlow, and Rianne Van Den Berg. 2021a. Structured denoising diffusion models in discrete state-spaces. *Advances in neural information processing systems*, 34:17981–17993.

Jacob Austin, Augustus Odena, Maxwell Nye, Maarten Bosma, Henryk Michalewski, David Dohan, Ellen Jiang, Carrie Cai, Michael Terry, Quoc Le, and 1 others. 2021b. Program synthesis with large language models. *arXiv preprint arXiv:2108.07732*.

Andrew Campbell, Joe Benton, Valentin De Bortoli, Thomas Rainforth, George Deligiannidis, and Arnaud Doucet. 2022. A continuous time framework for discrete denoising models. *Advances in Neural Information Processing Systems*, 35:28266–28279.

Huiwen Chang, Han Zhang, Lu Jiang, Ce Liu, and William T Freeman. 2022. Maskgit: Masked generative image transformer. In *Proceedings of the IEEE/CVF conference on computer vision and pattern recognition*, pages 11315–11325.

Mark Chen, Jerry Tworek, Heewoo Jun, Qiming Yuan, Henrique Ponde De Oliveira Pinto, Jared Kaplan, Harri Edwards, Yuri Burda, Nicholas Joseph, Greg Brockman, and 1 others. 2021. Evaluating large language models trained on code. *arXiv preprint arXiv:2107.03374*.

Shuang Cheng, Yihan Bian, Dawei Liu, Linfeng Zhang, Qian Yao, Zhongbo Tian, Wenhai Wang, Qipeng Guo, Kai Chen, Biqing Qi, and 1 others. 2025. Sdar: A synergistic diffusion-autoregression paradigm for scalable sequence generation. *arXiv preprint arXiv:2510.06303*.

Karl Cobbe, Vineet Kosaraju, Mohammad Bavarian, Mark Chen, Heewoo Jun, Lukasz Kaiser, Matthias Plappert, Jerry Tworek, Jacob Hilton, Reiichiro Nakano, and 1 others. 2021. Training verifiers to solve math word problems. *arXiv preprint arXiv:2110.14168*.

Leo Gao, Jonathan Tow, Baber Abbasi, Stella Biderman, Sid Black, Anthony DiPofi, Charles Foster, Laurence Golding, Jeffrey Hsu, Alain Le Noac’h, Haonan Li, Kyle McDonell, Niklas Muennighoff, Chris Ociepa, Jason Phang, Laria Reynolds, Hailey Schoelkopf, Aviya Skowron, Lintang Sutawika, and 5 others. 2024. [The language model evaluation harness](#).

Mor Geva, Daniel Khashabi, Elad Segal, Tushar Khot, Dan Roth, and Jonathan Berant. 2021. Did aristotle use a laptop? a question answering benchmark with implicit reasoning strategies. *Transactions of the Association for Computational Linguistics*, 9:346–361.

- Dan Hendrycks, Collin Burns, Saurav Kadavath, Akul Arora, Steven Basart, Eric Tang, Dawn Song, and Jacob Steinhardt. 2021. Measuring mathematical problem solving with the math dataset. *arXiv preprint arXiv:2103.03874*.
- Jonathan Ho, Ajay Jain, and Pieter Abbeel. 2020. Denoising diffusion probabilistic models. *Advances in neural information processing systems*, 33:6840–6851.
- Jonathan Ho, Tim Salimans, Alexey Gritsenko, William Chan, Mohammad Norouzi, and David J Fleet. 2022. Video diffusion models. *Advances in neural information processing systems*, 35:8633–8646.
- Emiel Hoogeboom, Didrik Nielsen, Priyank Jaini, Patrick Forré, and Max Welling. 2021. Argmax flows and multinomial diffusion: Learning categorical distributions. *Advances in neural information processing systems*, 34:12454–12465.
- Xiangqi Jin, Yuxuan Wang, Yifeng Gao, Zichen Wen, Biqing Qi, Dongrui Liu, and Linfeng Zhang. 2025. Thinking inside the mask: In-place prompting in diffusion llms. *arXiv preprint arXiv:2508.10736*.
- Tero Karras, Miika Aittala, Timo Aila, and Samuli Laine. 2022. Elucidating the design space of diffusion-based generative models. *Advances in neural information processing systems*, 35:26565–26577.
- Bumjun Kim, Dongjae Jeon, Dueun Kim, Wonje Jeung, and Albert No. 2025a. Rainbow padding: Mitigating early termination in instruction-tuned diffusion llms. *arXiv preprint arXiv:2510.03680*.
- Jaeyeon Kim, Kulin Shah, Vasilis Kontonis, Sham Kakade, and Sitan Chen. 2025b. Train for the worst, plan for the best: Understanding token ordering in masked diffusions. *arXiv preprint arXiv:2502.06768*.
- Junhoo Lee, Seungyeon Kim, and Nojun Kwak. 2025. Unlocking the potential of diffusion language models through template infilling. *arXiv preprint arXiv:2510.13870*.
- Pengxiang Li, Yefan Zhou, Dilxat Muhtar, Lu Yin, Shilin Yan, Li Shen, Soroush Vosoughi, and Shiwei Liu. 2025. Diffusion language models know the answer before decoding. *arXiv preprint arXiv:2508.19982*.
- Shufan Li, Konstantinos Kallidromitis, Hritik Bansal, Akash Gokul, Yusuke Kato, Kazuki Kozuka, Jason Kuen, Zhe Lin, Kai-Wei Chang, and Aditya Grover. 2026. Lavida: A large diffusion language model for multimodal understanding. *Advances in Neural Information Processing Systems*, 38:105101–105134.
- Hunter Lightman, Vineet Kosaraju, Yuri Burda, Harrison Edwards, Bowen Baker, Teddy Lee, Jan Leike, John Schulman, Ilya Sutskever, and Karl Cobbe. 2024. Let’s verify step by step. In *International Conference on Learning Representations*, volume 2024, pages 39578–39601.
- Aaron Lou, Chenlin Meng, and Stefano Ermon. 2023. Discrete diffusion modeling by estimating the ratios of the data distribution. *arXiv preprint arXiv:2310.16834*.
- Guanxi Lu, Hao Mark Chen, Yuto Karashima, Zhi-can Wang, Daichi Fujiki, and Hongxiang Fan. 2025. Adablock-dllm: Semantic-aware diffusion llm inference via adaptive block size. *arXiv preprint arXiv:2509.26432*.
- Pan Lu, Hritik Bansal, Tony Xia, Jiacheng Liu, Chunyuan Li, Hannaneh Hajishirzi, Hao Cheng, Kai-Wei Chang, Michel Galley, and Jianfeng Gao. 2024. Mathvista: Evaluating mathematical reasoning of foundation models in visual contexts. In *International Conference on Learning Representations*, volume 2024, pages 23439–23554.
- Ahmed Masry, Xuan Long Do, Jia Qing Tan, Shafiq Joty, and Enamul Hoque. 2022. Chartqa: A benchmark for question answering about charts with visual and logical reasoning. In *Findings of the association for computational linguistics: ACL 2022*, pages 2263–2279.
- Shen Nie, Fengqi Zhu, Zebin You, Xiaolu Zhang, Jingyang Ou, Jun Hu, Jun Zhou, Yankai Lin, Ji-Rong Wen, and Chongxuan Li. 2026. Large language diffusion models. *Advances in Neural Information Processing Systems*, 38:50608–50646.
- OpenAI. 2024. [Simple evals](#).
- Jingyang Ou, Shen Nie, Kaiwen Xue, Fengqi Zhu, Jiacheng Sun, Zhenguo Li, and Chongxuan Li. 2025. Your absorbing discrete diffusion secretly models the conditional distributions of clean data. In *International Conference on Learning Representations*, volume 2025, pages 64972–65009.
- William Peebles and Saining Xie. 2023. Scalable diffusion models with transformers. In *Proceedings of the IEEE/CVF international conference on computer vision*, pages 4195–4205.
- Subham S Sahoo, Marianne Arriola, Yair Schiff, Aaron Gokaslan, Edgar Marroquin, Justin T Chiu, Alexander Rush, and Volodymyr Kuleshov. 2024. Simple and effective masked diffusion language models. *Advances in Neural Information Processing Systems*, 37:130136–130184.
- Jiaxin Shi, Kehang Han, Zhe Wang, Arnaud Doucet, and Michalis Titsias. 2024. Simplified and generalized masked diffusion for discrete data. *Advances in neural information processing systems*, 37:103131–103167.
- Jascha Sohl-Dickstein, Eric Weiss, Niru Maheswaranathan, and Surya Ganguli. 2015. Deep unsupervised learning using nonequilibrium thermodynamics. In *International conference on machine learning*, pages 2256–2265. pmlr.

- Yang Song, Jascha Sohl-Dickstein, Diederik P Kingma, Abhishek Kumar, Stefano Ermon, and Ben Poole. 2020. Score-based generative modeling through stochastic differential equations. *arXiv preprint arXiv:2011.13456*.
- Yubo Wang, Xueguang Ma, Ge Zhang, Yuansheng Ni, Abhranil Chandra, Shiguang Guo, Weiming Ren, Aaran Arulraj, Xuan He, Ziyang Jiang, and 1 others. 2024. Mmlu-pro: A more robust and challenging multi-task language understanding benchmark. *Advances in Neural Information Processing Systems*, 37:95266–95290.
- Chengyue Wu, Hao Zhang, Shuchen Xue, Zhijian Liu, Shizhe Diao, Ligeng Zhu, Ping Luo, Song Han, and Enze Xie. 2025. Fast-dllm: Training-free acceleration of diffusion llm by enabling kv cache and parallel decoding. *arXiv preprint arXiv:2505.22618*.
- Zhen Xiong, Yujun Cai, Zhecheng Li, and Yiwei Wang. 2025. Unveiling the potential of diffusion large language model in controllable generation. *arXiv preprint arXiv:2507.04504*.
- Jiacheng Ye, Zhihui Xie, Lin Zheng, Jiahui Gao, Zirui Wu, Xin Jiang, Zhenguo Li, and Lingpeng Kong. 2025. Dream 7b: Diffusion large language models. *arXiv preprint arXiv:2508.15487*.
- Kaiwen Zheng, Yongxin Chen, Hanzi Mao, Ming-Yu Liu, Jun Zhu, and Qinsheng Zhang. 2025. Masked diffusion models are secretly time-agnostic masked models and exploit inaccurate categorical sampling. In *International Conference on Learning Representations*, volume 2025, pages 63186–63227.

## Contents

<b>A</b>	<b>Algorithm</b>	<b>13</b>
<b>B</b>	<b>Additional Experimental Details</b>	<b>13</b>
B.1	Models and Evaluation Splits . . .	13
B.2	Prompting and Evaluation Protocol	13
B.3	Hyperparameter Selection and Sensitivity Analysis . . . . .	13
<b>C</b>	<b>Additional Experiments</b>	<b>14</b>
C.1	Code-Generation Results . . . . .	14
C.2	Ablation Over Suffix Anchors . .	14
C.3	Ablation Over Anchor Positions .	14
<b>D</b>	<b>Qualitative Analysis</b>	<b>15</b>
D.1	Qualitative Comparison of Decoding Variants . . . . .	15
D.2	Decoding Progress and Confidence Dynamics . . . . .	15
<b>E</b>	<b>Use of LLMs in This Work</b>	<b>15</b>

## A Algorithm

Algorithm 1 summarizes the complete decoding procedure for Suffix-Anchored Confidence Modulation. Starting from a masked response sequence, our method first inserts a suffix anchor at predefined response positions and computes the anchor-proximity weights. At each decoding step, the underlying confidence-based strategy computes token predictions and confidence scores for the remaining masked positions. Our method then reweights these confidence scores according to anchor proximity and decoding progress, while leaving the base position-selection rule and token prediction rule unchanged.

## B Additional Experimental Details

### B.1 Models and Evaluation Splits

Benchmark	Hugging Face Identifier	Split	Size
GSM8K	openai/gsm8k	test	1,319
MATH-500	HuggingFaceH4/MATH-500	test	500
StrategyQA	ChilleD/StrategyQA	test	687
MMLU-Pro	TIGER-Lab/MMLU-Pro	test	12,032
MathVista	AI4Math/MathVista	testmini	1,000
ChartQA	HuggingFaceM4/ChartQA	test	2,500
HumanEval	openai/openai_humaneval	test	164
MBPP	google-research-datasets/mbpp	test	500

Table 8: **Evaluation datasets and splits.** Hugging Face identifiers, evaluation splits, and evaluation-set sizes used in our experiments. MathVista uses the testmini split because answer labels are not available for the test split.

We use the publicly available checkpoints GSAI-ML/LLaDA-8B-Instruct, Dream-org/Dream-v0-Instruct-7B, and jacklishufan/lavida-llada-v1.0-instruct for LLaDA 8B-Instruct, Dream 7B-Instruct, and LaViDa-Instruct, respectively. Table 8 summarizes the datasets, Hugging Face identifiers, evaluation splits, and evaluation-set sizes used in our experiments. We use the test split for all benchmarks except MathVista, for which we use the testmini split because answer labels are not provided for the test split.

### B.2 Prompting and Evaluation Protocol

We re-implement DLM evaluation on the reported benchmarks based on the evaluation setup of lm-evaluation-harness (Gao et al., 2024), simple-evals (OpenAI, 2024), and the LaViDa (Li et al., 2026) codebase. For multiple-choice benchmarks, we use generative evaluation: the model generates

a response, and the final answer is extracted from the generated text rather than selecting among answer candidates by log probability. For reasoning benchmarks, we include “*Let’s think step by step.*” at the end of the prompt to elicit reasoning before the final answer.

### B.3 Hyperparameter Selection and Sensitivity Analysis

Benchmark	$\kappa$	$\beta$	$\gamma$
GSM8K	14	1.3	0.85
MATH-500	12	1.5	0.85
StrategyQA	12	1.3	0.70
MMLU-Pro	14	1.3	0.85
MathVista	14	1.3	0.85
ChartQA	12	1.0	1.00
HumanEval	14	1.3	0.85
MBPP	14	1.5	0.70

Table 9: **Selected hyperparameters.** Hyperparameter values selected for each benchmark. The GSM8K setting is used for benchmarks without a training or validation split.

When a training or validation split is available, we select the hyperparameters  $(\kappa, \beta, \gamma)$  using a lightweight sweep over 128 randomly sampled examples. The sweep range is  $\kappa \in \{12, 14\}$ ,  $\beta \in \{1.0, 1.1, 1.2, 1.3, 1.4, 1.5\}$ , and  $\gamma \in \{0.7, 0.85, 1.0\}$ . The sweep is conducted with LLaDA 8B-Instruct under top-probability decoding, and the selected values are reused for top-margin decoding and Dream experiments on the same benchmark. For benchmarks without a training or validation split, we use the GSM8K setting. Table 9 reports the selected hyperparameters for each benchmark.

To assess sensitivity, we vary each hyperparameter around the GSM8K setting on a randomly sampled subset of 256 training examples, using LLaDA 8B-Instruct with top-probability decoding. For  $\kappa$  and  $\gamma$ , we additionally include values outside the selection sweep to test robustness to wider ranges. Table 10 shows that performance remains stable across a wide range of values. On the same subset, unmodified top-probability decoding and suffix anchoring alone obtain 15.63 and 55.86, respectively; all hyperparameter settings in Table 10 substantially exceed these scores. This suggests that the gains of our method do not rely on a narrowly tuned hyperparameter choice.

---

**Algorithm 1** Suffix-Anchored Confidence Modulation

---

**Require:** Model  $M_\theta$ , prompt  $\mathbf{x}_{\text{prompt}}$ , generation length  $L$ , decoding step budget  $T$

**Require:** Suffix anchor tokens  $\mathbf{x}_{\text{anchor}}$ , anchor positions  $\mathcal{A}$

**Require:** Base confidence function  $C(\cdot)$ , position-selection rule  $\text{Select}(\cdot)$

**Require:** Hyperparameters  $\kappa, \beta, \gamma$

- 1: Initialize  $\mathbf{x}^{(T)} \leftarrow \text{InsertAnchor}(\text{concat}(\mathbf{x}_{\text{prompt}}, [\text{MASK}]^L), \mathbf{x}_{\text{anchor}}, \mathcal{A})$
  - 2: Compute anchor-proximity weights for all response positions  $i$ :
  - 3:  $w_i \leftarrow \min \left\{ 1, \beta \max_{a \in \mathcal{A}} \exp \left( -\frac{|i-a|}{\kappa} \right) \right\}$
  - 4: **for**  $t = T, T-1, \dots, 1$  **do**
  - 5:  $\mathcal{M}^{(t)} \leftarrow \{i : x_i^{(t)} = [\text{MASK}]\}$
  - 6: Compute logits  $\mathbf{z}^{(t)} \leftarrow M_\theta(\mathbf{x}^{(t)})$
  - 7: Predict tokens  $\hat{\mathbf{x}}_0 \leftarrow \arg \max(\mathbf{z}^{(t)}, \dim = -1)$
  - 8: Compute base confidence scores  $c_i^{(t)} \leftarrow C(\mathbf{z}^{(t)}, i)$  for all  $i \in \mathcal{M}^{(t)}$
  - 9: Compute decoding progress  $p^{(t)} \leftarrow 1 - |\mathcal{M}^{(t)}|/L$
  - 10: Reweight confidence scores:
  - 11:  $\tilde{c}_i^{(t)} \leftarrow c_i^{(t)} (1 - w_i(1 - p^{(t)})^\gamma)$  for all  $i \in \mathcal{M}^{(t)}$
  - 12: Select positions to unmask  $\mathcal{U}^{(t)} \leftarrow \text{Select}(\{\tilde{c}_i^{(t)}\}_{i \in \mathcal{M}^{(t)}})$
  - 13: Update  $\mathbf{x}^{(t-1)} \leftarrow \mathbf{x}^{(t)}$
  - 14: Replace  $x_i^{(t-1)} \leftarrow \hat{x}_{0,i}$  for all  $i \in \mathcal{U}^{(t)}$
  - 15: **end for**
  - 16: **Return:** response segment of  $\mathbf{x}^{(0)}$
- 

## C Additional Experiments

### C.1 Code-Generation Results

Table 11 reports code-generation results on HumanEval and MBPP using LLaDA 8B-Instruct. The results show a trend consistent with the reasoning benchmarks: suffix anchoring improves both confidence-based decoding strategies, and adding confidence modulation on top of suffix anchoring further improves performance. Under top-probability decoding, the average pass@1 increases from 18.14 to 27.23 with suffix anchoring and further to 30.67 with the full method. Under top-margin decoding, the average pass@1 increases from 20.74 to 28.73 with suffix anchoring and further to 31.76 with the full method. These results indicate that the proposed method also extends to code generation, where suffix anchoring encourages response completion and confidence modulation helps mitigate premature decoding of anchor-adjacent code.

### C.2 Ablation Over Suffix Anchors

We ablate the choice of suffix anchor on GSM8K using LLaDA 8B-Instruct with top-probability decoding. In the main experiments, we use “*The answer is*” as the suffix anchor for reasoning bench-

marks. Table 12 compares this default anchor with several alternatives. Across all tested anchors, suffix anchoring substantially improves over the unmodified top-probability baseline, and adding confidence modulation on top of suffix anchoring consistently provides further gains. Notably, even the anchor “.”, which provides minimal response structure, improves the baseline from 14.94 to 54.13 with suffix anchoring and to 74.68 with the full method. This provides strong evidence that *the suffix anchor primarily acts as a lightweight continuation cue that encourages meaningful generation toward a later response region, rather than imposing a specific response template*. In this sense, suffix anchoring differs from prior DLM prompting strategies for controllable or structured generation that prescribe detailed response structures or output constraints (Xiong et al., 2025; Jin et al., 2025; Lee et al., 2025). Overall, the results show that our method remains effective across different suffix anchor choices, even when the anchor provides minimal response structure, such as “*is*”, “*,*”, or “*..*”.

### C.3 Ablation Over Anchor Positions

We ablate anchor positions on GSM8K using LLaDA 8B-Instruct with top-probability decoding

Varied	$\kappa$	$\beta$	$\gamma$	Accuracy
$\kappa$	6	1.3	0.85	73.83
	8	1.3	0.85	78.52
	10	1.3	0.85	76.96
	12	1.3	0.85	80.08
	<b>14</b>	<b>1.3</b>	<b>0.85</b>	<b>82.03</b>
	16	1.3	0.85	79.30
$\beta$	14	1.0	0.85	78.13
	14	1.1	0.85	77.74
	14	1.2	0.85	80.08
	<b>14</b>	<b>1.3</b>	<b>0.85</b>	<b>82.03</b>
	14	1.4	0.85	79.30
	14	1.5	0.85	80.47
$\gamma$	14	1.3	0.40	79.30
	14	1.3	0.55	80.47
	14	1.3	0.70	81.25
	<b>14</b>	<b>1.3</b>	<b>0.85</b>	<b>82.03</b>
	14	1.3	1.00	80.86
	14	1.3	1.15	78.52

Table 10: **Hyperparameter sensitivity on GSM8K.** Accuracy is measured on 256 randomly sampled training examples using LLaDA 8B-Instruct with top-probability decoding. Each hyperparameter is varied around the GSM8K setting  $(\kappa, \beta, \gamma) = (14, 1.3, 0.85)$ .

and generation length  $L = 256$ . Table 13 reports results for two suffix anchors, “*The answer is*” and the semantically minimal anchor “.”, while varying the insertion position within the later response region. The default position is  $-20$ , meaning 20 positions before the end of the response region, and the ablation moves the anchor earlier relative to this default position. Across both suffix anchors, the full method with confidence modulation remains robust across different anchor positions within the later response region. At the same time, as the anchor is moved to earlier positions, the EOT ratio in generated outputs tends to increase. This position-dependent change in EOT ratio supports our interpretation that the suffix anchor acts as a lightweight cue for response continuation toward a later response region, rather than imposing a fixed response template.

## D Qualitative Analysis

### D.1 Qualitative Comparison of Decoding Variants

Figures 4–11 provide qualitative comparisons among the unmodified confidence-based baseline, suffix anchoring, and the full method with confidence modulation. For each figure, the subfigures corresponding to these three decoding variants vi-

Model	Decoding Method	HumanEval	MBPP	Average
LLaDA	Random	18.90	22.40	20.65
	Top Probability	17.07	19.20	18.14
	+ Suffix Anchor	28.66	25.80	27.23
	+ Confidence Modulation	<b>32.93</b>	<b>28.40</b>	<b>30.67</b>
	Top Margin	17.07	24.40	20.74
	+ Suffix Anchor	28.66	28.80	28.73
	+ Confidence Modulation	<b>31.71</b>	<b>31.80</b>	<b>31.76</b>

Table 11: **Results on code-generation benchmarks.** Pass@1 (%) is reported on HumanEval and MBPP using LLaDA 8B-Instruct. For each confidence-based decoding strategy, the unmodified baseline, suffix anchoring, and the full method with confidence modulation are compared. Random position selection is included as a non-confidence-based reference. **Bold** indicates the best result within each confidence-based decoding group.

sualize confidence over token positions (left) and unmasked tokens (right) at the initial step and an intermediate decoding step, together with the final output (bottom). These examples illustrate how suffix anchoring mitigates incomplete generation, while confidence modulation reduces premature decoding near the suffix anchor.

### D.2 Decoding Progress and Confidence Dynamics

Figure 12 visualizes the decoding process of Suffix-Anchored Confidence Modulation on a GSM8K example using LLaDA 8B-Instruct with top-probability decoding. The figure shows confidence over token positions and the corresponding unmasked tokens from the initial step to the final decoding step. This illustrates how the method gradually resolves the response while progressively relaxing the confidence modulation near the suffix anchor, allowing anchor-adjacent positions to be decoded after more surrounding context has been generated.

## E Use of LLMs in This Work

LLM-based assistance was used during the preparation of this work. Specifically, LLMs were used to support code implementation and debugging, and to improve the clarity, grammar, and readability of the manuscript. All scientific ideas, methodological decisions, experimental analyses, and interpretations originated from the authors. Any code or text produced with LLM assistance was carefully reviewed, verified, and edited by the authors before being included in this work. The authors take full responsibility for the content of the manuscript.

Suffix Anchor	Decoding Method	Accuracy
No Suffix Anchor	Unmodified Top Probability	14.94
“The answer is” (Default)	Suffix Anchoring + Confidence Modulation	49.89 <b>76.88</b>
“Therefore, the answer is”	Suffix Anchoring + Confidence Modulation	52.77 <b>74.45</b>
“Answer:”	Suffix Anchoring + Confidence Modulation	49.58 <b>73.16</b>
“is”	Suffix Anchoring + Confidence Modulation	55.12 <b>73.62</b>
“ ”	Suffix Anchoring + Confidence Modulation	55.12 <b>73.77</b>
“.”	Suffix Anchoring + Confidence Modulation	54.13 <b>74.68</b>

Table 12: **Ablation over suffix anchors.** Accuracy (%) is reported on GSM8K using LLaDA 8B-Instruct with top-probability decoding. Each suffix anchor is inserted at the same anchor position before decoding begins. **Bold** indicates the best result within each suffix-anchor group.

Anchor Position	Decoding Method	Acc.	EOT Ratio
No Anchor	Unmodified Top Probability	14.94	0.66
-20 (Default)	Suffix Anchoring	49.89	0.05
	+ Confidence Modulation	76.88	0.05
-30	Suffix Anchoring	52.69	0.09
	+ Confidence Modulation	76.88	0.09
-40	Suffix Anchoring	55.04	0.13
	+ Confidence Modulation	76.65	0.13
-50	Suffix Anchoring	56.33	0.17
	+ Confidence Modulation	77.33	0.17
-60	Suffix Anchoring	56.48	0.21
	+ Confidence Modulation	74.68	0.21

(a) Suffix Anchor: “The answer is” (Default)

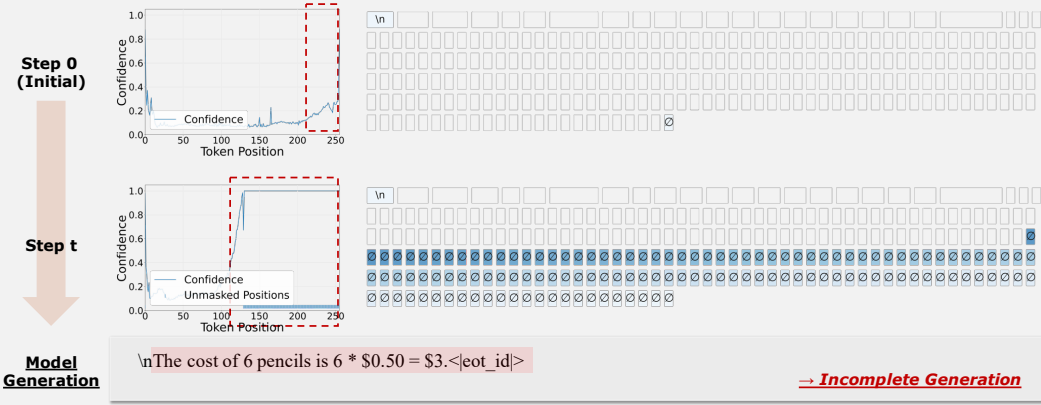
Anchor Position	Decoding Method	Acc.	EOT Ratio
No Anchor	Unmodified Top Probability	14.94	0.66
-20 (Default)	Suffix Anchoring	54.13	0.07
	+ Confidence Modulation	74.68	0.08
-30	Suffix Anchoring	56.18	0.11
	+ Confidence Modulation	75.06	0.12
-40	Suffix Anchoring	56.48	0.15
	+ Confidence Modulation	74.37	0.15
-50	Suffix Anchoring	55.72	0.19
	+ Confidence Modulation	74.91	0.19
-60	Suffix Anchoring	56.94	0.23
	+ Confidence Modulation	73.31	0.23

(b) Suffix Anchor: “.”

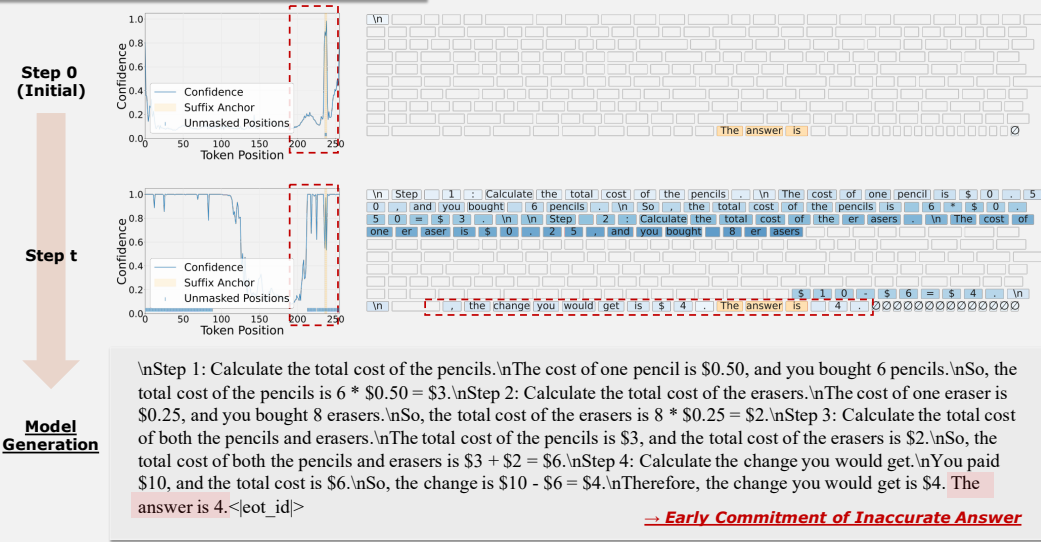
Table 13: **Ablation over anchor positions.** Accuracy (%) and EOT ratio are reported on GSM8K using LLaDA 8B-Instruct with top-probability decoding and generation length  $L = 256$ . Anchor position  $-k$  denotes inserting the suffix anchor  $k$  positions before the end of the response region.

**Question :** A pencil cost \$0.50, and an eraser cost \$0.25. If you bought 6 pencils and 8 erasers and paid \$10, how much change would you get?  
**Reference Answer :** 5

**Top-Probability Decoding**



**Top-Probability Decoding + Suffix Anchor**



**Top-Probability Decoding + Suffix Anchor + Confidence Modulation**

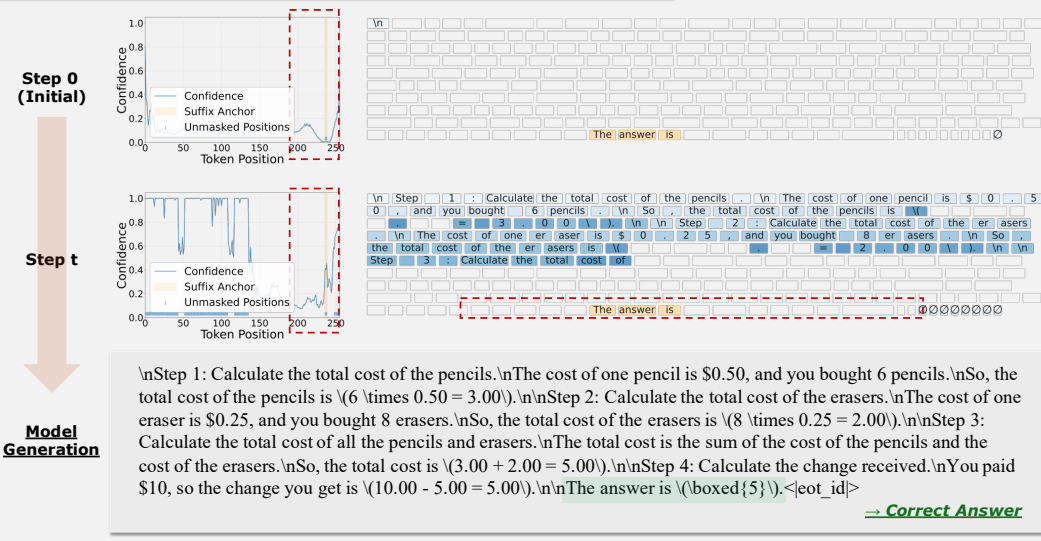
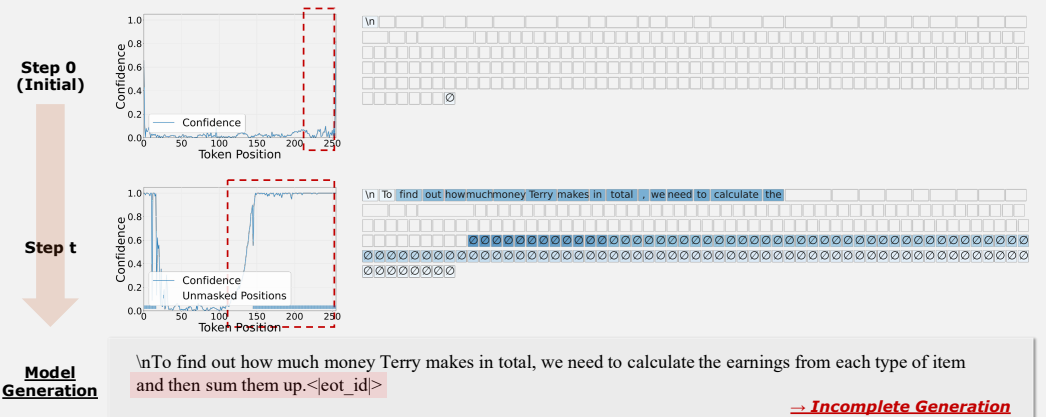


Figure 4: **Qualitative example on GSM8K under top-probability decoding.** The unmodified baseline, suffix anchoring, and the full method with confidence modulation are compared using LLaDA. It shows confidence over token positions and unmasked tokens at the initial step and an intermediate decoding step, along with the final output. Darker blue token boxes indicate positions decoded at later steps.  $\emptyset$  denotes the `<|endof text|>` token.

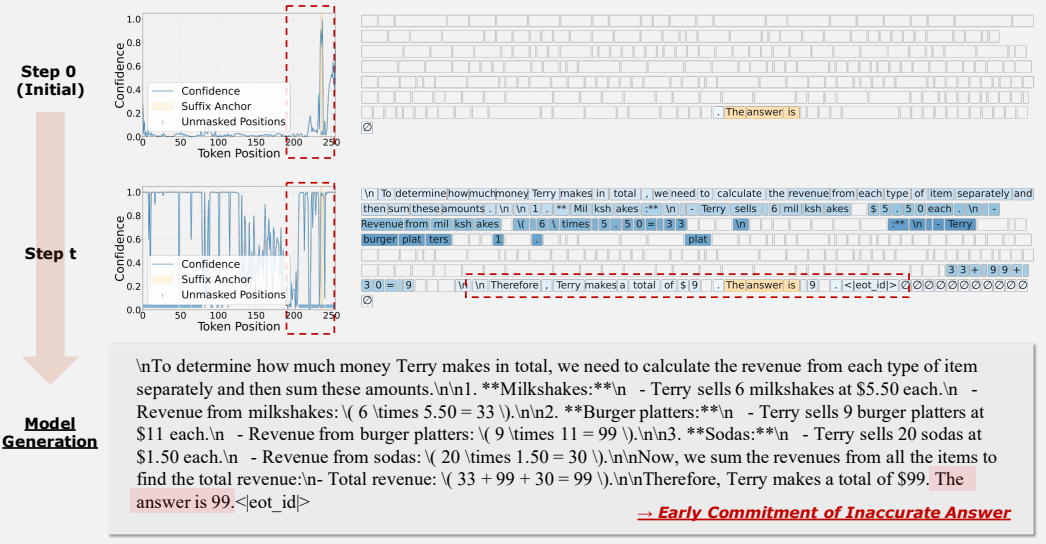
**Question :** Terry sells 6 milkshakes for \$5.50 each, nine burger platters for \$11 each, and 20 sodas for \$1.50 each. How much money does he make in total?

**Reference Answer :** 162

**Top-Margin Decoding**



**Top-Margin Decoding + Suffix Anchor**



**Top-Margin Decoding + Suffix Anchor + Confidence Modulation**

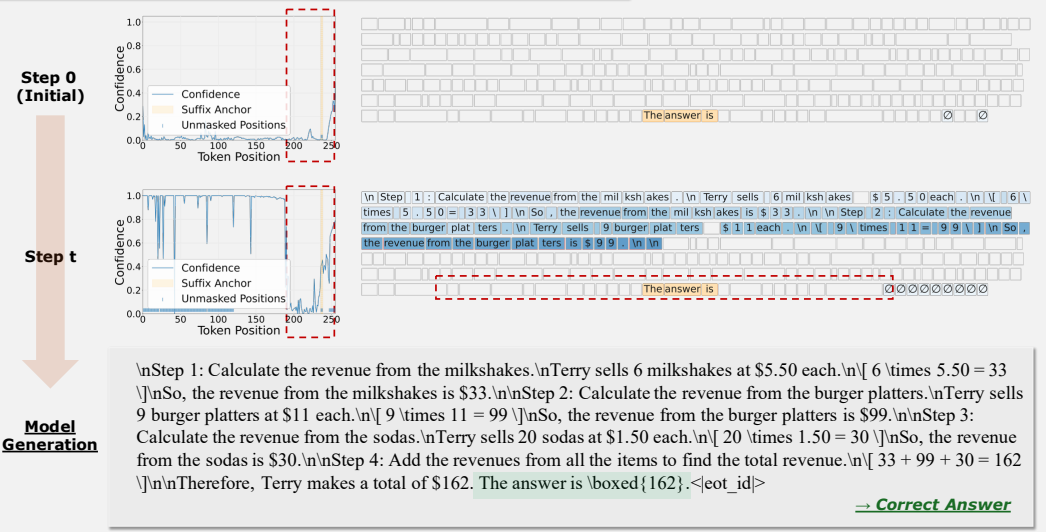
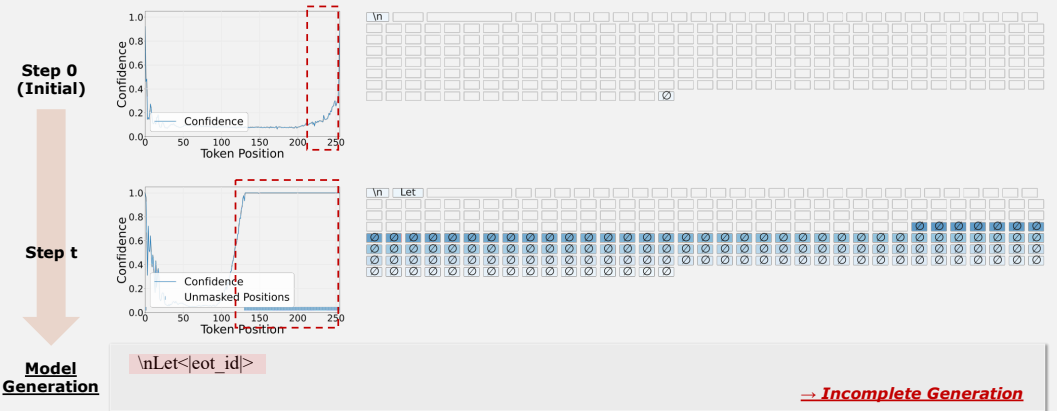


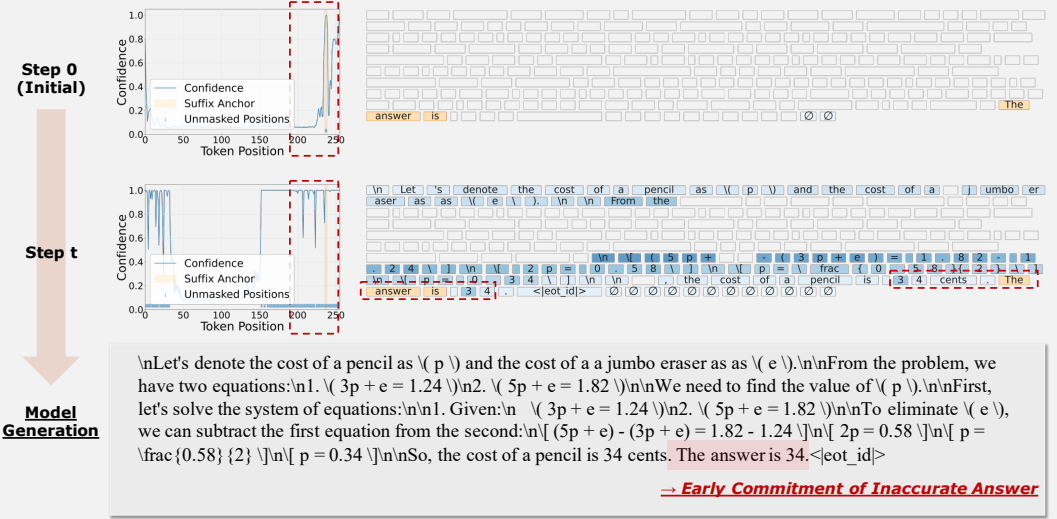
Figure 5: Qualitative example on GSM8K under top-margin decoding. The unmodified baseline, suffix anchoring, and the full method with confidence modulation are compared using LLaDA. It shows confidence over token positions and unmasked tokens at the initial step and an intermediate decoding step, along with the final output. Darker blue token boxes indicate positions decoded at later steps. ∅ denotes the <|endof'text'|> token.

**Question :** Three pencils and a jumbo eraser cost  $\$1.24$ . Five pencils and a jumbo eraser cost  $\$1.82$ . No prices include tax. In cents, what is the cost of a pencil?  
**Reference Answer :** 29

**Top-Probability Decoding**



**Top-Probability Decoding + Suffix Anchor**



**Top-Probability Decoding + Suffix Anchor + Confidence Modulation**

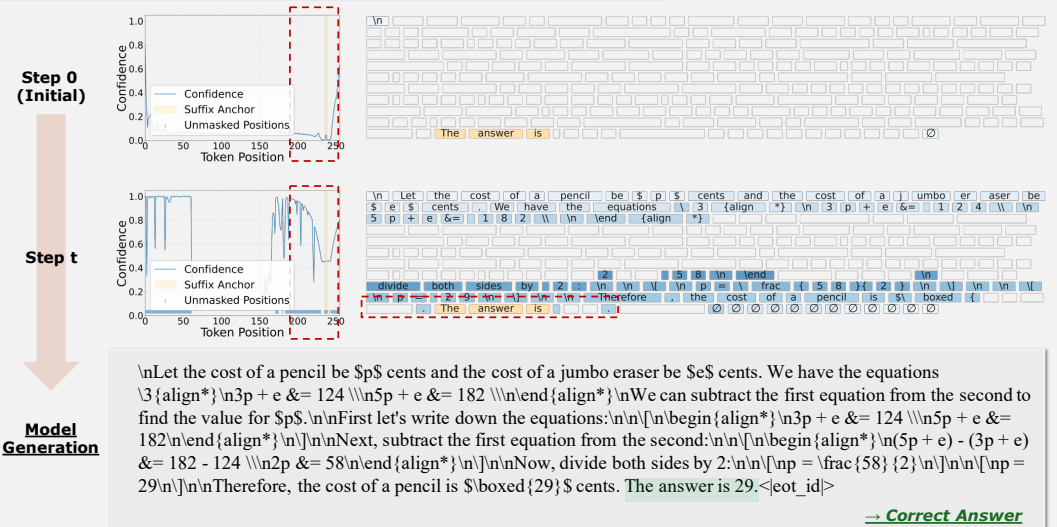
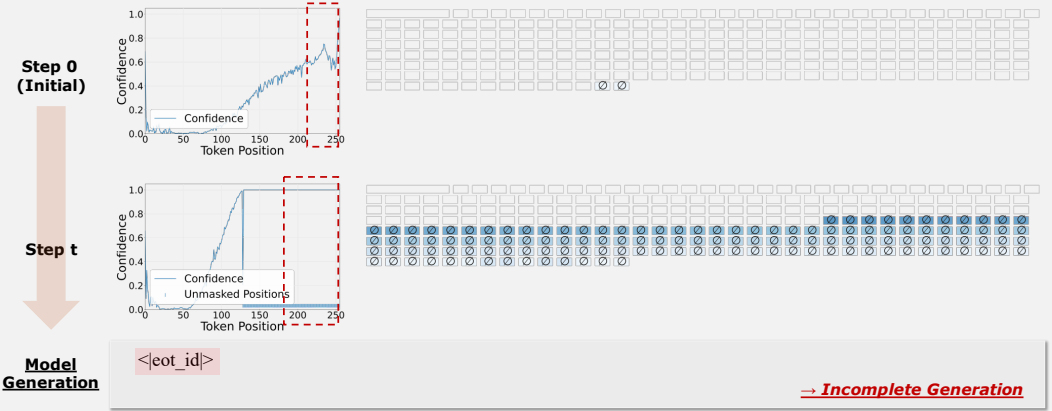


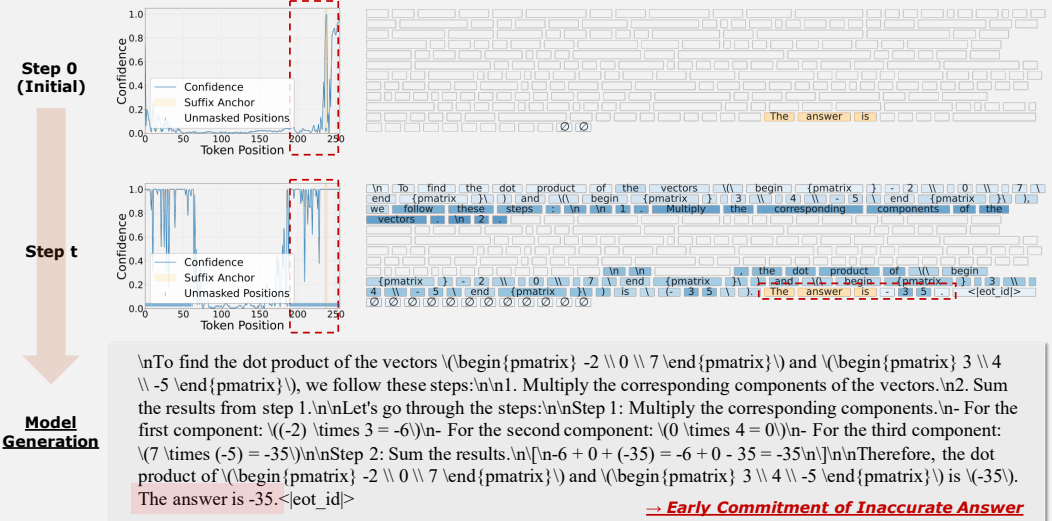
Figure 6: **Qualitative example on MATH-500 under top-probability decoding.** The unmodified baseline, suffix anchoring, and the full method with confidence modulation are compared using LLaDA. It shows confidence over token positions and unmasked tokens at the initial step and an intermediate decoding step, along with the final output. Darker blue token boxes indicate positions decoded at later steps.  $\emptyset$  denotes the  $\langle \text{end of text} \rangle$  token.

Question : Find the dot product of  $\begin{pmatrix} -2 \\ 0 \\ 7 \end{pmatrix}$  and  $\begin{pmatrix} 3 \\ 4 \\ -5 \end{pmatrix}$ .  
 Reference Answer : **-41**

**Top-Margin Decoding**



**Top-Margin Decoding + Suffix Anchor**



**Top-Margin Decoding + Suffix Anchor + Confidence Modulation**

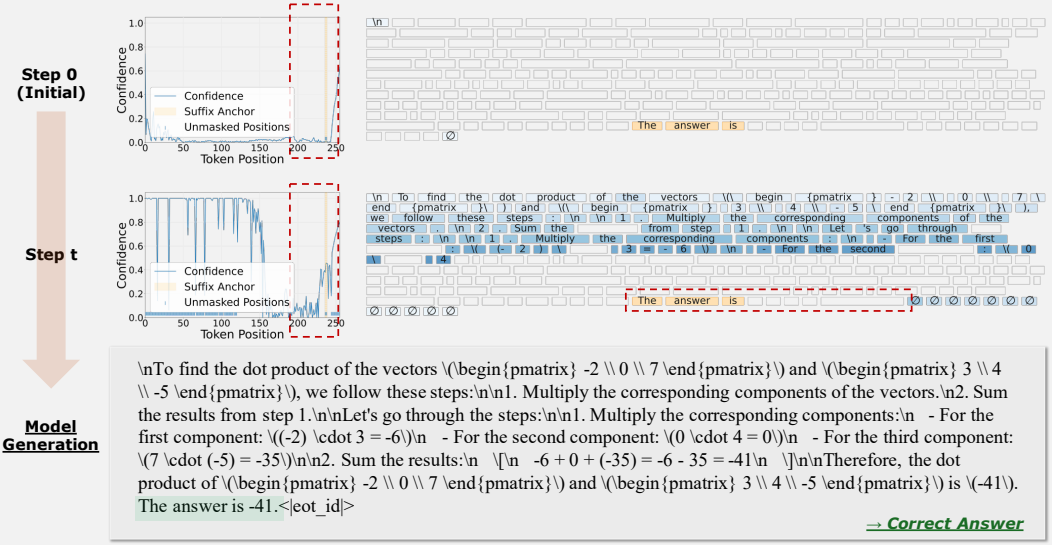
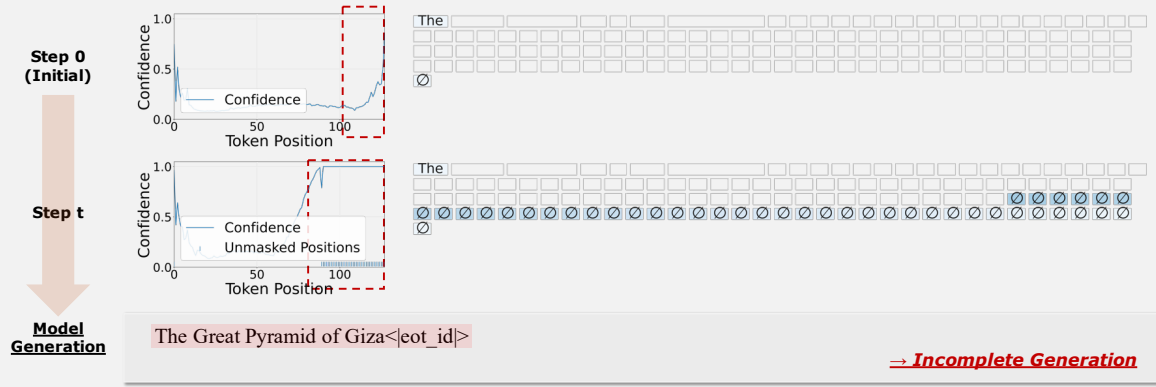


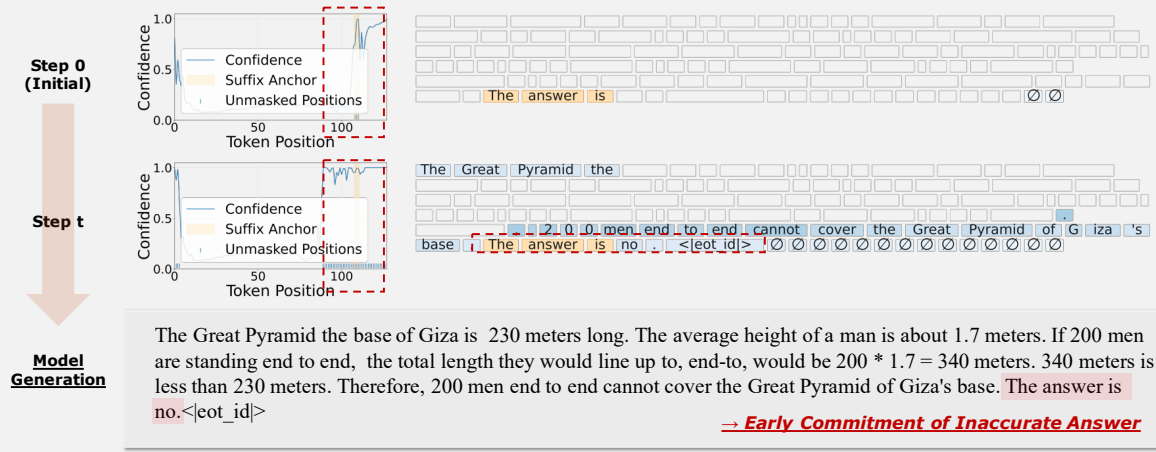
Figure 7: **Qualitative example on MATH-500 under top-margin decoding.** The unmodified baseline, suffix anchoring, and the full method with confidence modulation are compared using LLaDA. It shows confidence over token positions and unmasked tokens at the initial step and an intermediate decoding step, along with the final output. Darker blue token boxes indicate positions decoded at later steps.  $\emptyset$  denotes the  $\langle \text{end of text} \rangle$  token.

Question : Can 200 men end to end cover Great Pyramid of Giza's base?  
 Reference Answer : **yes**

**Top-Probability Decoding**



**Top-Probability Decoding + Suffix Anchor**



**Top-Probability Decoding + Suffix Anchor + Confidence Modulation**

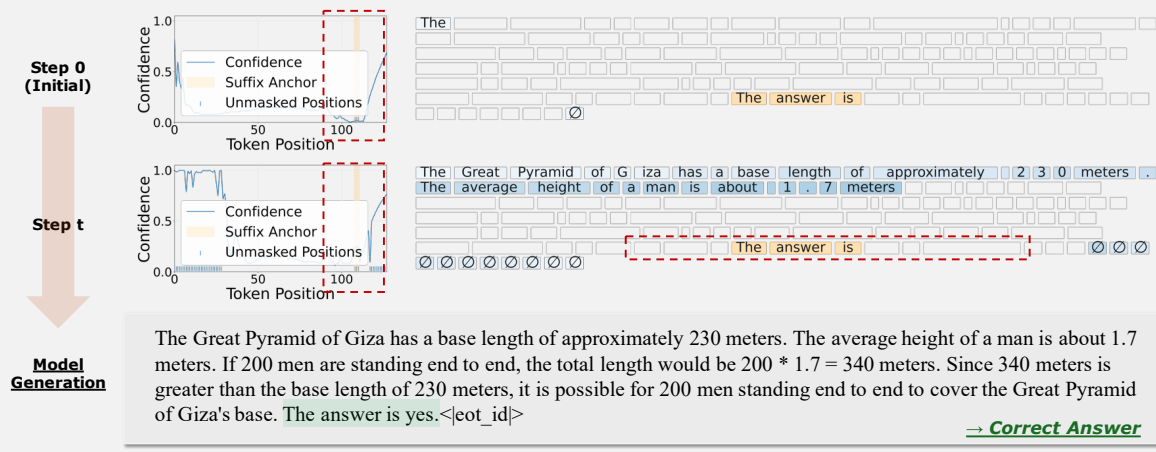
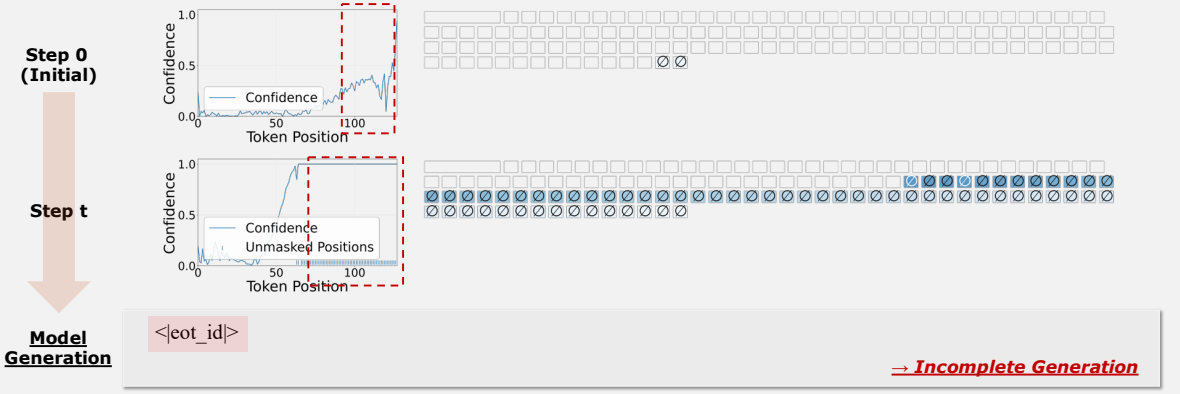


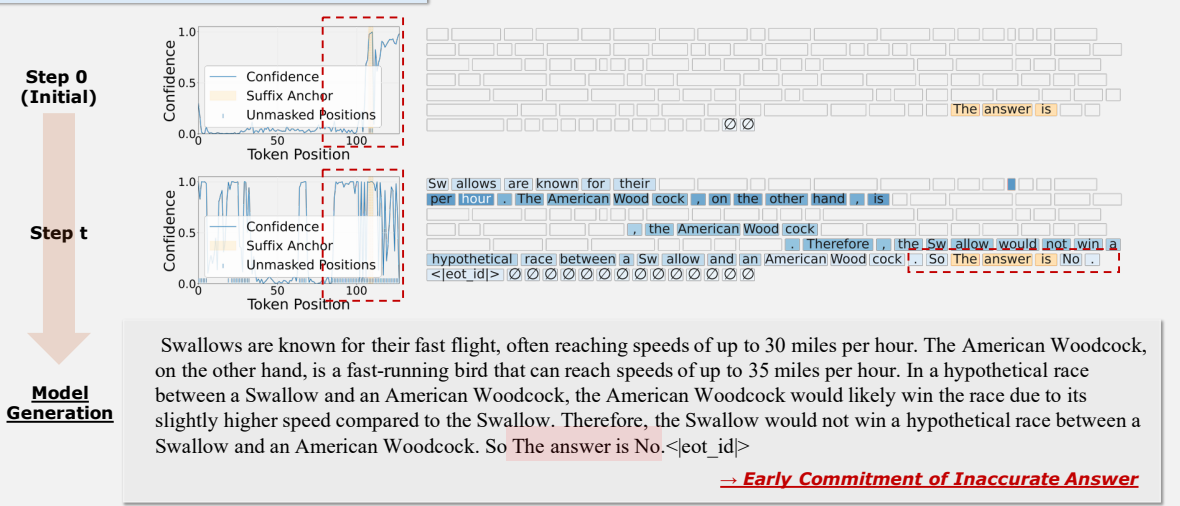
Figure 8: **Qualitative example on StrategyQA under top-probability decoding.** The unmodified baseline, suffix anchoring, and the full method with confidence modulation are compared using LLaDA. It shows confidence over token positions and unmasked tokens at the initial step and an intermediate decoding step, along with the final output. Darker blue token boxes indicate positions decoded at later steps. ∅ denotes the <|eot\_text|> token.

Question : In a hypothetical race between a Swallow and an American Woodcock, would the Swallow win?  
 Reference Answer : **yes**

**Top-Margin Decoding**



**Top-Margin Decoding + Suffix Anchor**



**Top-Margin Decoding + Suffix Anchor + Confidence Modulation**

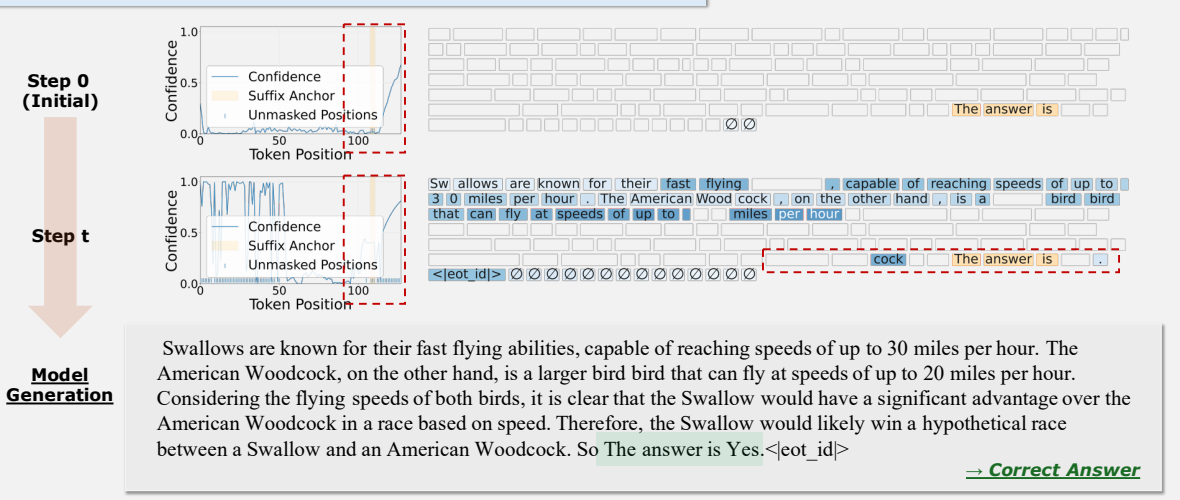
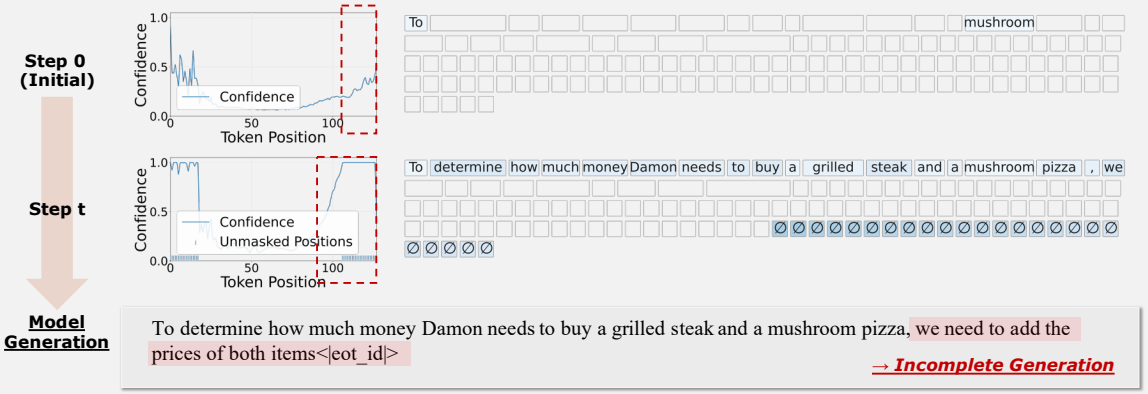


Figure 9: **Qualitative example on StrategyQA under top-margin decoding.** The unmodified baseline, suffix anchoring, and the full method with confidence modulation are compared using LLaDA. It shows confidence over token positions and unmasked tokens at the initial step and an intermediate decoding step, along with the final output. Darker blue token boxes indicate positions decoded at later steps. ∅ denotes the <|endoftext|> token.

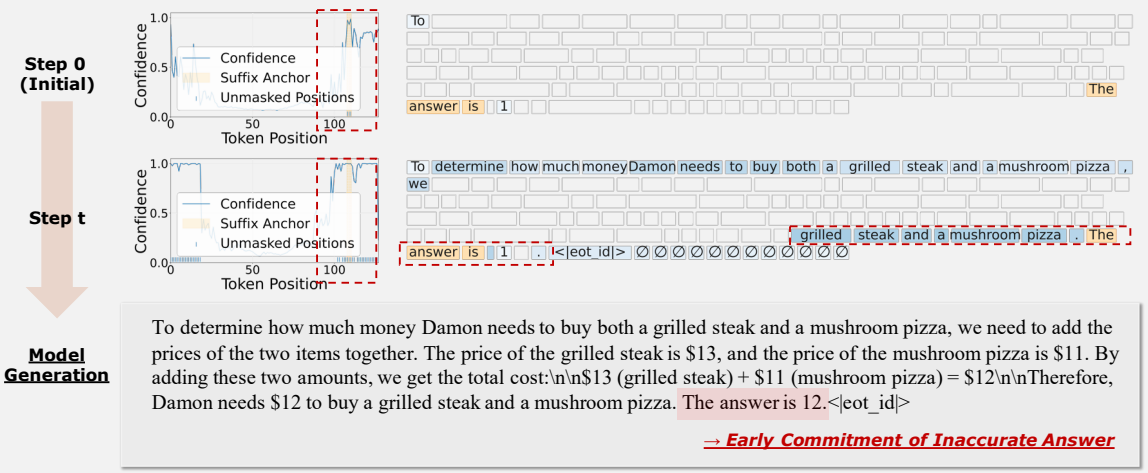
Question : How much money does Damon need to buy a grilled steak and a mushroom pizza? (Unit: \$)  
 Reference Answer : 24

pasta with white sauce	\$15
mushroom pizza	\$11
grilled steak	\$13
pasta with meat sauce	\$12

### Top-Probability Decoding



### Top-Probability Decoding + Suffix Anchor



### Top-Probability Decoding + Suffix Anchor + Confidence Modulation

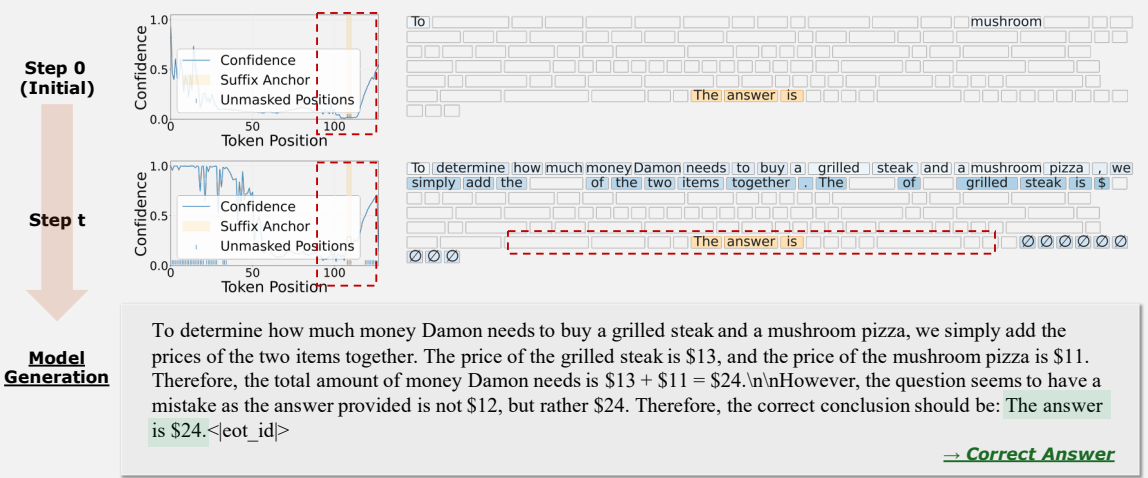
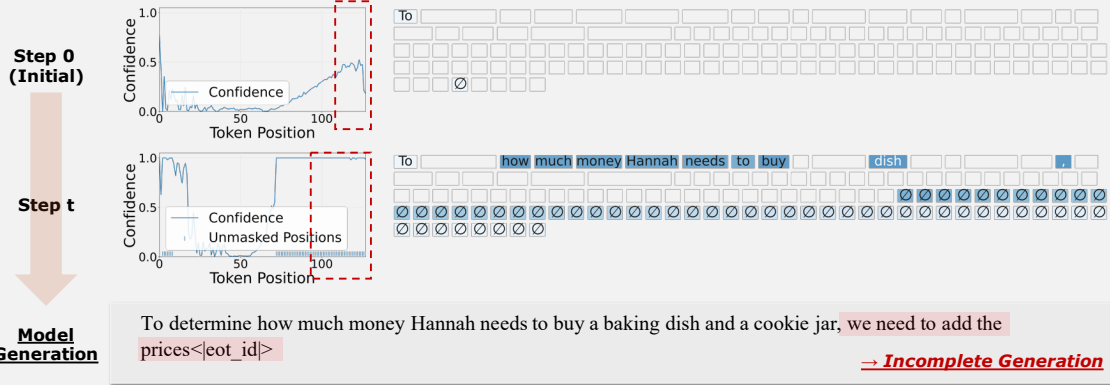


Figure 10: **Qualitative example on MathVista under top-probability decoding.** The unmodified baseline, suffix anchoring, and the full method with confidence modulation are compared using LaViDa. It shows confidence over token positions and unmasked tokens at the initial step and an intermediate decoding step, along with the final output. Darker blue token boxes indicate positions decoded at later steps.  $\emptyset$  denotes the  $\langle | \text{endof text} | \rangle$  token.

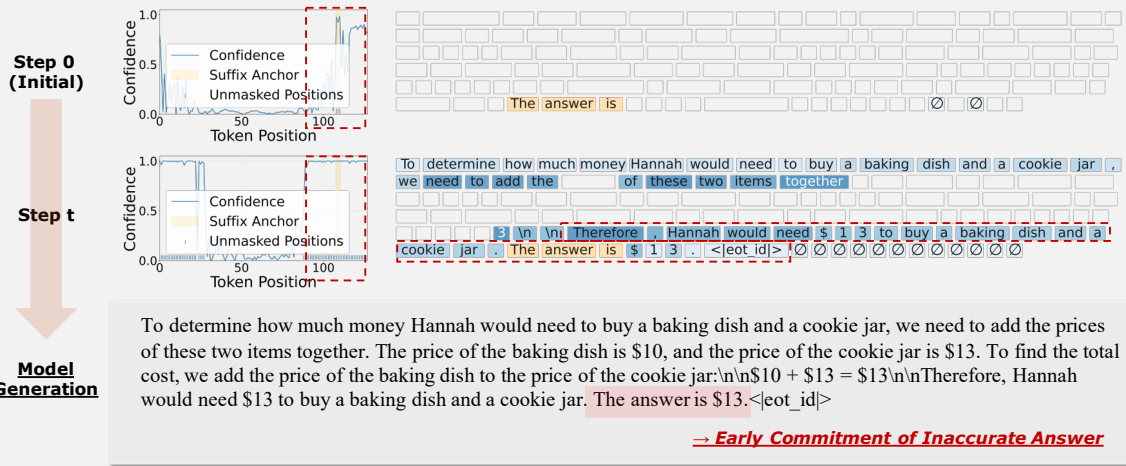
Question : How much money does Hannah need to buy a baking dish and a cookie jar? (Unit: \$)  
 Reference Answer : 23

frying pan	\$48
baking dish	\$10
casserole dish	\$13
cookie jar	\$13
rolling pin	\$15

### Top-Margin Decoding



### Top-Margin Decoding + Suffix Anchor



### Top-Margin Decoding + Suffix Anchor + Confidence Modulation

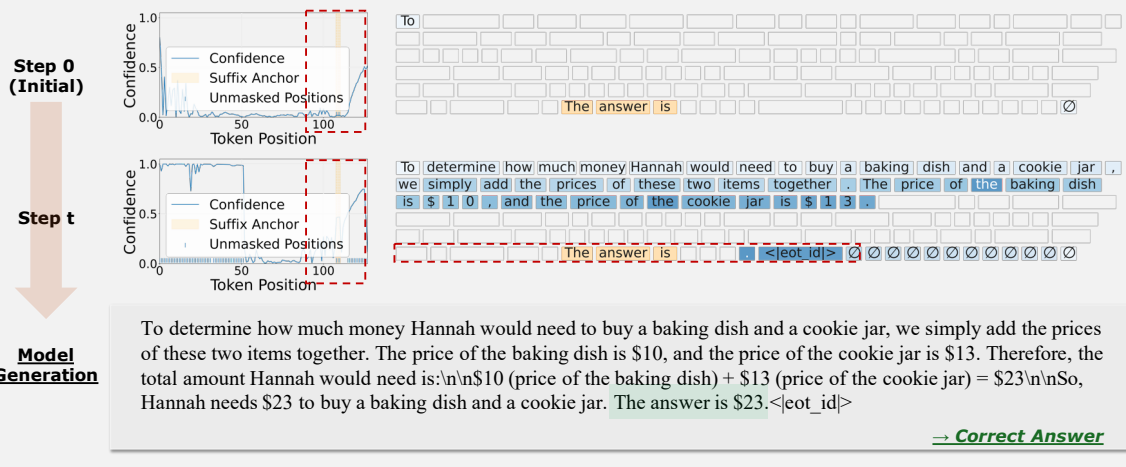


Figure 11: **Qualitative example on MathVista under top-margin decoding.** The unmodified baseline, suffix anchoring, and the full method with confidence modulation are compared using LaViDa. It shows confidence over token positions and unmasked tokens at the initial step and an intermediate decoding step, along with the final output. Darker blue token boxes indicate positions decoded at later steps. ∅ denotes the <|endof text|> token.

**Question :** Kris is trying to earn a video game achievement for playing a total of 30 hours. If Kris plays for half an hour every day for 2 weeks then plays for 2 hours every day for a week, how many hours does she still need to play to earn the achievement?

**Reference Answer :** 9

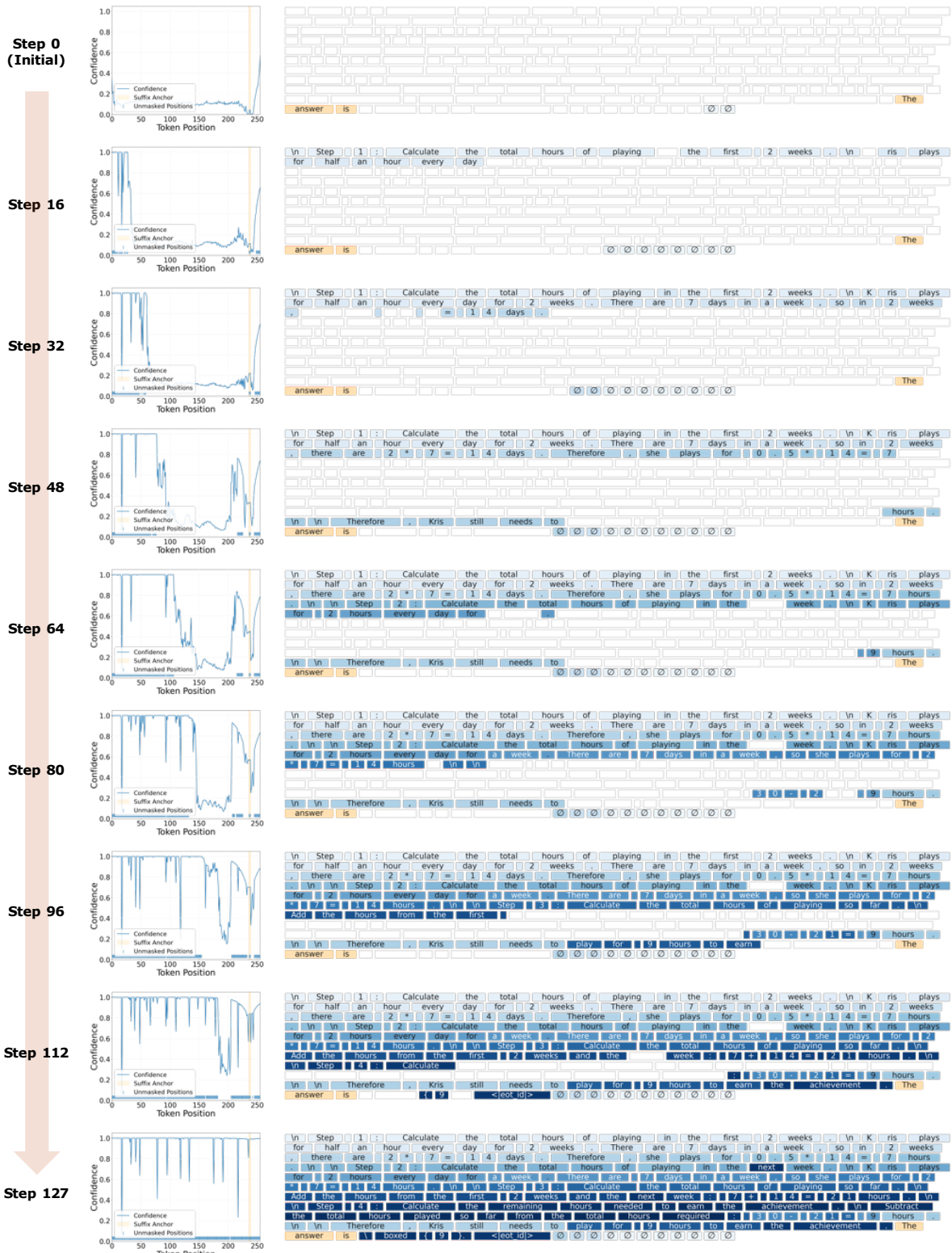


Figure 12: Decoding progress of Suffix-Anchored Confidence Modulation. Confidence over token positions (left) and unmasked tokens (right) are visualized from the initial step to the final decoding step for a GSM8K example using LLaDA under top-probability decoding. Darker blue token boxes indicate positions decoded at later steps.  $\emptyset$  denotes the  $\langle \text{end of text} \rangle$  token.